



HHS Public Access

Author manuscript

Cell Rep. Author manuscript; available in PMC 2021 November 09.

Published in final edited form as:

Cell Rep. 2021 October 05; 37(1): 109785. doi:10.1016/j.celrep.2021.109785.

Serum- and glucocorticoid-induced kinase drives hepatic insulin resistance by directly inhibiting AMP-activated protein kinase

Ben Zhou^{1,2,3,4,*}, Yuyao Zhang^{1,2,3}, Sainan Li^{1,2,3}, Lianfeng Wu⁵, Geza Fejes-Toth⁶, Aniko Naray-Fejes-Toth⁶, Alexander A. Soukas^{1,2,3,7,*}

¹Department of Medicine, Diabetes Unit and Center for Genomic Medicine, Massachusetts General Hospital, Boston, MA 02114, USA

²Department of Medicine, Harvard Medical School, Boston, MA 02114, USA

³Broad Institute of Harvard and MIT, Cambridge, MA 02142, USA

⁴CAS Key Laboratory of Nutrition, Metabolism and Food Safety, Shanghai Institute of Nutrition and Health, University of Chinese Academy of Sciences, Chinese Academy of Sciences, Shanghai, 200031, China

⁵Institute of Basic Medical Sciences, Westlake Institute for Advanced Study, School of Life Sciences, Westlake University, Hangzhou, 310024, China

⁶Department of Molecular and Systems Biology, Geisel School of Medicine at Dartmouth, Hanover, NH, 03755, USA

⁷Lead contact

SUMMARY

A hallmark of type 2 diabetes (T2D) is hepatic resistance to insulin's glucose-lowering effects. The serum- and glucocorticoid-regulated family of protein kinases (SGK) is activated downstream of mechanistic target of rapamycin complex 2 (mTORC2) in response to insulin in parallel to AKT. Surprisingly, despite an identical substrate recognition motif to AKT, which drives insulin sensitivity, pathological accumulation of SGK1 drives insulin resistance. Liver-specific *Sgk1*-knockout (*Sgk1*^{L^{ko}}) mice display improved glucose tolerance and insulin sensitivity and are protected from hepatic steatosis when fed a high-fat diet. *Sgk1* promotes insulin resistance by inactivating AMP-activated protein kinase (AMPK) via phosphorylation on inhibitory site

This is an open access article under the CC BY-NC-ND license (<http://creativecommons.org/licenses/by-nc-nd/4.0/>).

*Correspondence: benzhou@sibs.ac.cn (B.Z.), asoukas@mgh.harvard.edu (A.A.S.).

AUTHOR CONTRIBUTIONS

Conceptualization, B.Z. and A.A.S.; Methodology, B.Z., L.W. Y.Z., S.L., and A.A.S.; Formal Analysis, B.Z. and A.A.S.; Investigation, B.Z., L.W., and A.A.S.; Resources, G.F.-T. and A.N.-F.-T.; Writing – Original Draft, B.Z. and A.A.S.; Writing – Review & Editing, B.Z. and A.A.S.; Visualization, B.Z. and A.A.S.; Supervision, A.A.S.; Funding Acquisition, A.A.S.

DECLARATION OF INTERESTS

The authors declare no competing interests.

INCLUSION AND DIVERSITY

We worked to ensure sex balance in the selection of non-human subjects. While citing references scientifically relevant for this work, we also actively worked to promote gender balance in our reference list.

SUPPLEMENTAL INFORMATION

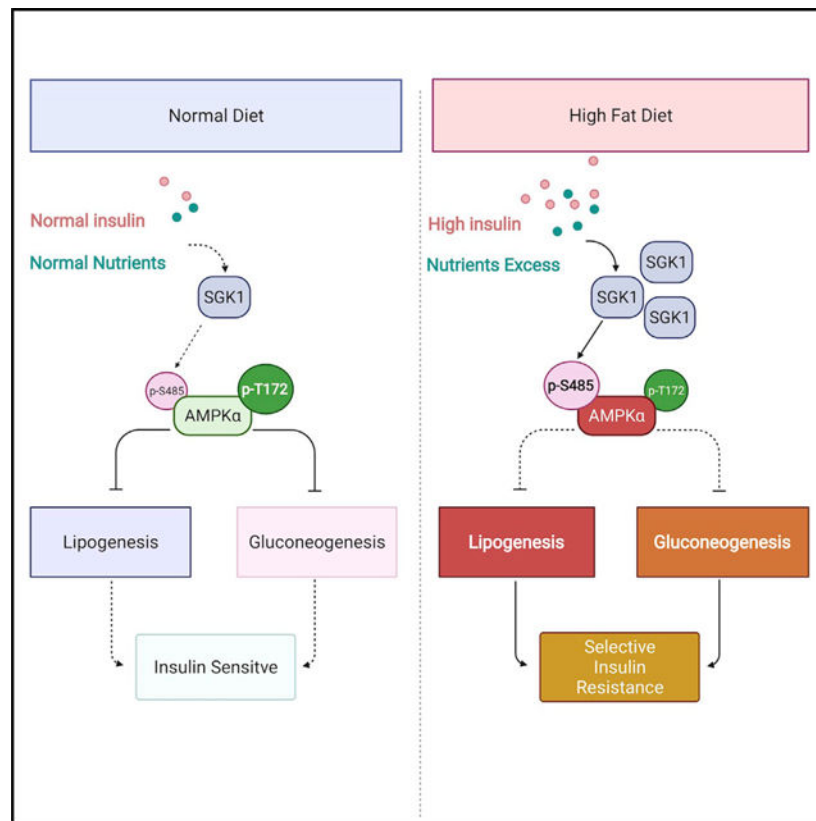
Supplemental information can be found online at <https://doi.org/10.1016/j.celrep.2021.109785>.

AMPK α ^{Ser485/491}. We demonstrate that SGK1 is dominant among SGK family kinases in regulation of insulin sensitivity, as *Sgk1*, *Sgk2*, and *Sgk3* triple-knockout mice have similar increases in hepatic insulin sensitivity. In aggregate, these data suggest that targeting hepatic SGK1 may have therapeutic potential in T2D.

In brief

The insulin-activated serine/threonine kinase serum- and glucocorticoid-induced kinase 1 (SGK1) phosphorylates an identical substrate recognition motif to Akt. Here, Zhou et al. show that, in contrast to Akt, HFD-induced SGK1 overactivation promotes insulin resistance in liver by phosphorylating and inhibiting the activity of AMP-activated protein kinase.

Graphical Abstract



INTRODUCTION

A central feature of type 2 diabetes (T2D) is resistance to the antihyperglycemic properties of insulin (Czech, 2017). This manifests as a reduction in phosphorylation of the insulin receptor substrates (IRS) and Akt in hepatocytes, resulting in less effective suppression of hepatic glucose output by insulin (Petersen and Shulman, 2018). Emerging data support several hypotheses as to the mechanism of insulin resistance in T2D. One hypothesis is that phospholipases prompt accumulation of diacylglycerol, activating atypical protein kinase C (PKC) to phosphorylate and desensitize the insulin receptor (Samuel et al., 2004). A second

hypothesis is that inflammation associated with accumulation of cellular lipids activates insulin resistance through pathways such as endoplasmic reticulum (ER) stress, c-Jun N-terminal kinase (JNK), and inhibitor of kappa B kinase-nuclear factor kappa B (IKK-NF κ B) signaling (Rondinone, 2007). Third, but by no means last, is the idea that nutrient (e.g., amino acids, glucose, fatty acids) and energy (ATP) excess activates mechanistic target of rapamycin complex 1 (mTORC1) and the lipogenic transcription factors carbohydrate response element binding protein (ChREBP) and sterol response element binding protein 1c (SREBP-1c), concomitantly suppressing the catabolism-promoting energy sensor AMP-activated protein kinase (AMPK) (Guo, 2014). The net consequence of these effects is negative feedback on proximal insulin signaling and further accumulation of metabolites that inhibit insulin signaling, such as triglycerides (TGs) and free fatty acids.

These mechanisms are indirect, mediated by accumulation of lipids or free or esterified fatty acids or by parallel activation of stress and inflammatory pathways. Alternatively, early insulin resistance may be promoted directly by events proximal to and directly affected by insulin signaling, for example, negative feedback on insulin signaling by mTORC1 mediated by phosphorylation of Grb10 by mTORC1 and of IRS1^{Ser302} by the mTORC1 effector S6 kinase (S6K) (Haruta et al., 2000; Hsu et al., 2011; Yu et al., 2011). However, the importance of IRS1^{Ser302} phosphorylation by S6K has been called into question on the basis of normal glucose homeostasis in IRS1^{Ser302Ala}-knockin mice (Copps et al., 2016). Thus, additional IRS1 phosphorylation events or other activities of mTORC1 may be required for negative feedback on insulin signaling.

The heteromultimeric protein kinase mTORC2, which contains mTOR but is structurally and mechanistically distinct from mTORC1, is a critical component of insulin signaling in liver (Hagiwara et al., 2012; Lamming et al., 2012; Yuan et al., 2012). Insulin signaling activates mTORC2 through phosphoinositide 3-kinase (PI3K) (Liu et al., 2015), and mTORC2 in turn phosphorylates and activates protein kinase A, protein kinase G, PKC (AGC) family kinases such as AKT (Sarbasov et al., 2005), and serum- and glucocorticoid-regulated kinase (SGK) (García-Martínez and Alessi, 2008).

Mammalian genomes harbor three genes encoding SGK family members: *Sgk1*, *Sgk2*, and *Sgk3* (Kobayashi et al., 1999). All mammalian SGK isoforms possess conserved activation loop and C-terminal hydrophobic motif sites that are phosphorylated by PDK1 and mTORC2, respectively, upon stimulation of insulin and PI3K signaling (García-Martínez and Alessi, 2008; Unger and Zhou, 2001). *In vitro*, SGK phosphorylates an identical substrate recognition motif to Akt (Arg-X-Arg-X-X-Ser/Thr, where X represents any amino acid and Ser/Thr the phosphorylated residue), including bona fide Akt targets in gain-of-function experiments such as FoxO (Brunet et al., 2001; Sommer et al., 2013). However, emerging data suggest roles for SGK family kinases distinct from Akt.

AMPK is a heterotrimeric (consisting of catalytic α and regulatory β and γ subunits), a central regulator of anabolic and catabolic processes in response to cellular energy levels. Under low-energy states, such as fasting, activation of AMPK suppresses lipid and glycogen synthesis and enhances whole-body utilization of fat stores. Conversely, under energy-replete conditions, AMPK activity is reduced, stimulating anabolic and reducing catabolic

processes (Viollet et al., 2009b). These conclusions are supported by gain- and loss-of-function models in mice *in vivo*. Constitutive pharmacologic or genetic activation of hepatic AMPK leads to leanness, increases in long-chain fatty acid oxidation, increased ketogenesis, relative hypoglycemia, and improvement in insulin sensitivity (Andreelli et al., 2006; Esquejo et al., 2018; Viana et al., 2006; Yang et al., 2008). Liver-specific AMPK activation reduces liver steatosis and decreases expression of inflammatory genes in the context of diet-induced obesity (Garcia et al., 2019; Woods et al., 2017). Conversely, liver-specific AMPK α 2-knockout mice are hyperglycemic, hyperinsulinemic, and hypertriglyceridemic and have low fasting ketone levels, indicative of insulin resistance and defects in hepatic fatty acid oxidation and ketogenesis (Andreelli et al., 2006). However, contrasting data in liver-specific AMPK α 1 α 2-knockout mice, which demonstrate normal glucose homeostasis and insulin sensitivity, indicate that the regulation of energy homeostasis by AMPK is complex and context dependent (Foretz et al., 2010; Zhao et al., 2020).

AMPK activity is regulated by phosphorylation at Thr¹⁷² on its catalytic α 1/ α 2 subunits (Hardie, 2003). Conversely, phosphorylation of AMPK α 1^{Ser485} or AMPK α 2^{Ser491} has been shown to negatively regulate AMPK activity directly or by prompting ubiquitination and degradation of AMPK α (Jiang et al., 2021; Viollet et al., 2009b). Insulin is well known to decrease AMPK activity in hepatocytes (Witters and Kemp, 1992), but it remains unclear how insulin inhibits AMPK. A compelling possibility is that this occurs via phosphorylation of AMPK α 1^{Ser485} and AMPK α 2^{Ser491} by insulin-activated AGC family kinases. Three kinases, Akt, p70-S6K, and protein kinase A, have been reported to phosphorylate AMPK α subunits on these residues (Hardie, 2014).

Here, we report that SGK1 promotes insulin resistance by directly phosphorylating AMPK α ^{Ser485/491}, thereby inhibiting AMPK. Conversely, liver-specific knockout of *Sgk1* (*Sgk1*^{Lko}) protects against high-fat diet (HFD)-induced fatty liver and insulin resistance. Mice entirely lacking all three *Sgk* genes in liver (liver-specific *Sgk1* knockout in the background of whole-body *Sgk2* and *Sgk3* knockouts [*Sgk*^{Ltko}]) do not exhibit further improvement in insulin sensitivity, suggesting that *Sgk1* is dominant among the *Sgk* family members in governance of hepatic insulin action. Insulin sensitivity in *Sgk1*^{Lko} mice is mimicked by liver-specific expression of mutant, non-phosphorylatable AMPK α 1^{Ser485Ala} *in vivo*. In aggregate, these data indicate that SGK function promotes insulin resistance downstream of PI3K and mTORC2 signaling, predominantly by phosphorylating AMPK α ^{Ser485/491}, mitigating its favorable effects on insulin sensitivity.

RESULTS

Insulin resistance is associated with increased SGK1 protein levels

In order to test whether *Sgk1* associates with insulin resistance, we measured kinase levels in models of insulin resistance. First, in mice made insulin resistant by HFD feeding, hepatic SGK1 protein abundance is significantly higher after overnight fasting and refeeding compared with mice fed a normal chow diet (Figure 1A). Second, basal and insulin-stimulated SGK1 activity is elevated in insulin resistance induced by 12 weeks of HFD versus chow feeding, using the phosphorylation status of SGK1 substrate NDRG1^{T346} in liver as a proxy for kinase activity (Figure 1B). We validated this result in a second,

distinct cohort of mice fed HFD for 20 weeks, finding that although insulin-stimulated phosphorylation of NDRG1^{T346} by SGK1 is preserved in HFD feeding, phosphorylation of Akt^{S473} is attenuated (Figure 1C). Third, SGK1 protein increases significantly in mouse primary hepatocytes with palmitate treatment (Figure 1D), an *in vitro* model of insulin resistance (Ruddock et al., 2008). *Sgk1* mRNA levels in mice fed HFD and palmitate-treated hepatocytes are minimally elevated (Figures S1A and S1B), suggesting that insulin resistance governs SGK1 levels posttranscriptionally. Taken together, these data suggest that SGK1 protein levels and activity positively correlate with hepatic insulin resistance.

***Sgk1*^{Lko} mice exhibit increased hepatic insulin sensitivity**

To determine whether the increases in SGK1 activity are causal in insulin resistance (versus the downstream consequence of insulin resistance), we generated mice lacking *Sgk1* exclusively in the liver. Liver-specific *Sgk1*-knockout mice (genotype *Sgk1*^{flox/flox}; *Alb-Cre*^{Tg/0}, hereafter referred to as *Sgk1*^{Lko}) are viable, fertile, and born at expected Mendelian frequency. In all subsequent experiments, littermates without the albumin *Cre* transgene (genotype *Sgk1*^{flox/flox}) are used as controls. Knockout of hepatic *Sgk1* was confirmed by western blotting in isolated primary hepatocytes (Figure 1E). When fed normal chow, *Sgk1*^{Lko} mice and control mice have equivalent body mass, fat mass, lean mass, liver weight, food intake, and fasting serum glucose and insulin levels at 18 weeks of age (Figures S1C–S1I). There are no significant differences in glucose and insulin tolerance between control and *Sgk1*^{Lko} mice (Figures S1J and S1K).

Although *Sgk1*^{Lko} mice demonstrate no differences in glucose tolerance, *Sgk1*^{Lko} mice maintain euglycemia following a glucose challenge with significantly lower plasma insulin levels (Figure S1L), suggesting increased insulin sensitivity. Indeed, insulin-induced phosphorylation of AKT on both threonine 308 and serine 473 and FoxO1 on threonine 24 are all higher in the liver of *Sgk1*^{Lko} mice *in vivo* versus controls (Figure 1F). Consistent with cell-autonomous action of SGK1, insulin-stimulated AKT phosphorylation is also higher in primary hepatocytes from *Sgk1*^{Lko} mice (Figure 1G). Murine AML12 hepatocytes lacking functional SGK1 by CRISPR-Cas9 gene editing also show higher insulin-stimulated phosphorylation of Akt^{Thr308/Ser473} (Figure S1M). Finally, supporting the idea that activation of SGK can promote insulin resistance, expression of constitutively active SGK1^{Ser422Asp} decreases insulin-stimulated Akt phosphorylation in primary hepatocytes (Figure 1H).

***Sgk1*^{Lko} mice are resistant to HFD-induced insulin resistance, glucose intolerance, and fatty liver**

Given that hepatic insulin sensitivity is increased in *Sgk1*^{Lko} mice, we hypothesized that these mice may be resistant to HFD-induced glucose intolerance. Although fasting glucose and insulin levels are not different between control and *Sgk1*^{Lko} mice fed HFD (Figures S2A and S2B), when challenged with an intraperitoneal (i.p.) glucose load, male and female *Sgk1*^{Lko} mice demonstrate significant improvement in glucose tolerance (Figures 2A, 2B, and S2C). Similarly, lower blood glucose levels are found in *Sgk1*^{Lko} mice challenged with i.p. pyruvate (Figure 2C). Confirming heightened insulin sensitivity, following an i.p. insulin tolerance test, glucose levels are significantly lower in *Sgk1*^{Lko} mice versus controls (with

and without accounting for differences in baseline glucose; Figures 2D, 2E, S2E, and S2F). In concert with these physiological results, insulin-stimulated AKT^{T308/S473} phosphorylation in liver *in vivo* is significantly increased in HFD-fed *Sgk1*^{Lko} mice versus controls (Figure 2F).

Sgk1^{Lko} mice are protected against HFD-induced adiposity and fatty liver, exhibiting significant decreases in body fat mass, liver weight, liver TG, liver cholesterol, and serum cholesterol compared with control mice (Figures 3A–3D and S3E). There are no differences in lean mass, body weight, food intake, and serum TG level (Figures S3A–S3D). In aggregate, these data substantiate two important conclusions: (1) loss of function in SGK1 selectively promotes insulin's antihyperglycemic effects without promoting its lipogenic effects, and (2) because the insulin-sensitizing effects of *Sgk1* loss of function are evident even on a chow diet (Figure 1F), on which differences in fat mass are not evident (Figures S1C, S1D, and S1F), the mechanism of insulin sensitization is likely to be distinct from a simple reduction in hepatic or whole-body lipid content.

As *Sgk1*^{Lko} mice have improved glucose tolerance when fed HFD, we next compared expression of hepatic gluconeogenic genes in control versus *Sgk1*^{Lko} mice. Expression of gluconeogenic glucose-6-phosphatase (*G6pase*) mRNA is decreased in *Sgk1*^{Lko} liver in the fasted state (Figure 3E), and *G6pase* and phosphoenolpyruvate carboxykinase (*Pepck*), but not PPAR γ coactivator 1 α (*Pgc-1 α*) mRNAs are decreased in *Sgk1*^{Lko} primary hepatocytes (Figure 3F). In concert, basal and stimulated glucose output is significantly reduced in primary hepatocytes from *Sgk1*^{Lko} versus control mice (Figure 3G).

We next used indirect calorimetry in order to determine the mechanism for reduced fat mass in *Sgk1*^{Lko} mice fed HFD. Increased locomotory activity, oxygen consumption, CO₂ production, and heat production are evident in *Sgk1*^{Lko} mice (Figures S3F–S3J), suggesting that, in the absence of differences in food intake, increased energy expenditure accounts for decreased fat mass in *Sgk1*^{Lko} mice. Hepatic mRNAs *Fasn* (fatty acid synthase), *Scd1* (stearoyl-CoA desaturase), and *Srebp1c* are all reduced in *Sgk1*^{Lko} mice versus controls (Figure 3H), suggesting a parallel reduction in *de novo* lipogenesis. *Mcad* mRNA level is increased in *Sgk1*^{Lko} mice, suggesting increased fatty acid oxidation (Figure 3I). A commensurate decrease in mTORC1 signaling, a driver both of hepatic lipogenesis and insulin resistance (Khamzina et al., 2005), is evident in the liver of *Sgk1*^{Lko} mice (Figure 3J). Taken together, loss of hepatic *Sgk1* protects against HFD-induced steatosis and weight gain, likely through an increase in energy expenditure and fatty acid oxidation, and parallel decreases in lipogenic gene expression and pro-lipogenic mTORC1 signaling.

SGK1 phosphorylates AMPK α ^{Ser485/491}, inhibiting its activity

Hepatic insulin sensitivity, glucose metabolism, and lipid metabolism are regulated by nutrient-sensing pathways including opposing activities of AMPK and mTORC1. mTORC1 signaling is reduced in *Sgk1*^{Lko} mice (Figure 3J). One potential explanation for this decrease could be an increase in AMPK activity. Phosphorylation of AMPK α ^{Thr172} and ACC1^{Ser79}, a canonical AMPK substrate, is increased in the liver of *Sgk1*^{Lko} mice compared with control mice under fasting conditions (Figure 4A) and in *Sgk1*^{Lko} primary hepatocytes under serum

starvation (Figures 4B and 4C). These data suggest an inverse relationship between the activities of SGK1 and AMPK.

AMPK α associates with SGK1 by co-immunoprecipitation when co-expressed in 293T cells (Figure 4D). To ask whether SGK1 can directly phosphorylate AMPK, we carried out an *in vitro* kinase assay by incubating two different SGK1 isoforms with AMPK α 1 purified from 293T cells. Following electrophoretic separation of reaction products on a Phos-Tag gel, an upward-shifted band is evident by western blotting with anti-total AMPK α antibody, indicative of direct phosphorylation by SGK1 (Figure 4E).

We next asked whether SGK1 can inhibit AMPK by phosphorylating AMPK α ^{Ser485/491} (S485 for AMPK α 1 and S491 for AMPK α 2), as has been reported for other AGC family kinases PKA, AKT and S6K (Dagon et al., 2012; Djouder et al., 2010; Horman et al., 2006). We incubated two different SGK1 protein isoforms with recombinant, purified AMPK representing the most common heterotrimeric complex in liver, AMPK α 2 β 1 γ 1, in an *in vitro* kinase assay. By western blotting with a phospho-specific antibody, we found that SGK1 directly and robustly phosphorylates AMPK α 2^{Ser491} *in vitro* (Figure 4F).

We then determined whether SGK1 also phosphorylates AMPK α *in vivo*. In *Sgk1*^{Lko} primary hepatocytes, levels of phospho-AMPK α ^{Ser485/491} are decreased ~50% under both vehicle and insulin treatment conditions, while the phosphorylation of AMPK α ^{Thr172}, AKT^{Thr308}, and AKT^{Ser473} as well as phosphorylation of the AMPK target ACC1^{Ser79} were all upregulated compared with control hepatocytes (Figure 4G). Conversely, expression of constitutively active SGK1^{Ser422Asp} significantly increased levels of phospho-AMPK α ^{Ser485/491}, leading to a marked decrease in phosphorylated ACC1^{Ser79} (Figure S4A). Taken together, these data suggest that SGK1 acts as a major inhibitory kinase for AMPK by phosphorylating AMPK α ^{Ser485/491}.

Hepatic expression of AMPK α ^{Ser485Ala} improves glucose homeostasis and insulin sensitivity

To investigate the consequences of AMPK α ^{Ser485/491} phosphorylation on hepatic insulin sensitivity and glucose homeostasis *in vivo*, we generated adeno-associated virus (AAV) serotype 2/9 expressing GFP (control) versus mutant AMPK α 1^{Ser485Ala} lacking the SGK1-targeted, negative regulation site under the liver-specific thyroid binding globulin (TBG) promoter (Bell et al., 2011a, 2011b; Chen et al., 2013; Yan et al., 2012). Mice were fed HFD for 8 weeks and then transduced with AAV-AMPK α 1^{Ser485Ala} or AAV-GFP by tail vein injection. There are no differences in body weight, lean mass, fat mass, serum cholesterol, and liver weight manifest after 8 weeks of AMPK α 1^{Ser485Ala} expression (Figures S5A–S5E). However, glucose tolerance is improved and hepatic and serum TG levels are significantly reduced in AMPK α 1^{Ser485Ala}-transduced animals (Figures 5A–5C). Mice expressing AMPK α 1^{Ser485} exhibit increased insulin-stimulated hepatic Akt phosphorylation and increased FoxO1 phosphorylation (required for the antihyperglycemic effects of insulin) but increased AMPK-mediated inhibitory phosphorylation of Raptor^{S792} and decreased overall mTORC1 activity (required for the lipogenic effects of insulin) (Figures 5D and 5E). These data parallel our data in *Sgk1*^{Lko} mice, which have increased Akt-FoxO

phosphorylation (Figures 1F, 1G, and 2F) and decreased mTORC1 activity in liver *in vivo* (Figure 3J).

Knockout of hepatic SGK1 improves glucose homeostasis through AMPK

To determine whether SGK1 regulates hepatic insulin sensitivity through AMPK, we treated both wild-type and *Sgk1*^{Lko} primary hepatocytes with the AMPK inhibitor Compound C (Liu et al., 2014b). Inhibition of AMPK eliminates both the decreased glucose output and increased insulin-stimulated AKT phosphorylation evident in *Sgk1*^{Lko} hepatocytes (Figures 6A and 6B). Furthermore, wild-type primary hepatocytes expressing adenovirally delivered AMPK α 2^{Ser491Ala}, which lacks the putative AMPK α phosphorylation site, exhibit increased phosphorylation of AMPK α ^{Thr172} and Akt^{Thr308/Ser473} versus hepatocytes expressing control AMPK α 2 (Figure 6C). In contrast, *Sgk1*^{Lko} primary hepatocytes demonstrate a constitutive increase in phospho-AMPK α ^{Thr172} and Akt^{Thr308/Ser473} that is not further increased by expression of AMPK α 2^{Ser491Ala} (Figure 6C).

To investigate whether SGK1 also regulates hepatic glucose homeostasis and insulin sensitivity through AMPK *in vivo*, we injected male *Sgk1*^{Lko} mice and control mice fed HFD for 8 weeks with AAV2/9 expressing GFP or AMPK α 1^{Ser485Ala} under the liver-specific TBG promoter. Glucose tolerance tests 8 weeks after transduction indicate that expression of AMPK α 1^{Ser485Ala} significantly improved glucose tolerance versus GFP expression in control mice, validating our earlier result (Figures 5A and 6D). In contrast, glucose tolerance is improved in *Sgk1*^{Lko} mice, and there is no significant difference between knockout mice expressing GFP and AMPK α 1^{Ser485Ala} (Figure 6D). Similar results are evident in an insulin tolerance test, in which expression of AMPK α 1^{Ser485Ala} significantly increases insulin sensitivity in control mice but does not additively augment the already increased insulin sensitivity evident in *Sgk1*^{Lko} mice (Figure 6E). In keeping with the increase in *in vivo* insulin sensitivity, expression of AMPK α 1^{Ser485Ala} increases insulin-stimulated FoxO1 and AKT phosphorylation in control mice but does not further increase already elevated levels evident in *Sgk1*^{Lko} mice (Figure 6F). At least one mechanism by which SGK1 deficiency may improve insulin sensitivity is by reducing mTORC1 activity, thereby lowering negative feedback on insulin signaling. This is most likely mediated by decreased AMPK α ^{Ser485/491} phosphorylation in *Sgk1*^{Lko} mice, as expression of AMPK α 1^{Ser485Ala} decreases mTORC1 activity in the liver of control mice but does not further decrease the already reduced activity in *Sgk1*^{Lko} mice (Figure 6G). In aggregate, these data indicate that hepatic knockout of *Sgk1* improves insulin sensitivity and glucose tolerance in an AMPK-dependent manner.

Regulation of glucose homeostasis by SGK family members

The three SGK family members have highly homologous kinase domains and share common substrates (Böhmer et al., 2004). Similar to SGK1, we find increased SGK2 and SGK3 protein levels in the liver of mice fed HFD (Figure 7A). To study the function of all SGK family members in liver, we first generated *Sgk2* and *Sgk3* global knockout mice (*Sgk2*^{-/-} and *Sgk3*^{-/-}) using CRISPR-Cas9 zygotic injection in C57BL/6N embryos. After four backcrosses to C57BL/6J mice, glucose and insulin tolerance in male *Sgk2*^{-/-} and *Sgk3*^{-/-} mice fed a normal chow diet are not significantly different versus wild-type mice (Figures

S6A–S6D). On HFD, at 17 weeks of age, one cohort of *Sgk2*^{-/-} knockout mice exhibited a slight but significant improvement of glucose tolerance but not insulin tolerance (Figures S6E and S6F), whereas a second cohort at 26 weeks of age showed no difference (Figures S6G and S6H). Two independent cohorts of *Sgk3*-knockout mice show mild improvement in HFD-induced insulin resistance but not glucose intolerance (Figures S6I–S6L).

To investigate whether there is functional redundancy among SGK1, SGK2, and SGK3 in the liver, we crossed *Sgk2*^{-/-};*Sgk3*^{-/-} global knockout mice with *Sgk1*^{Lko} mice to generate mice lacking hepatic expression of all *Sgk* family members (*Sgk*^{Ltko}), confirmed by western blotting in primary hepatocytes (Figure 7B). *Sgk*^{Ltko} hepatocytes have significantly increased hepatic AKT phosphorylation levels versus control hepatocytes (Figure 7C), suggesting increased hepatic insulin sensitivity. Similar to single *Sgk1*^{Lko} mice, no significant differences were found in glucose and insulin tolerance on a normal chow diet (Figures S6M and S6N). Similar to single *Sgk1*^{Lko} mice, *Sgk*^{Ltko} mice are resistant to HFD-induced glucose intolerance but not insulin resistance (Figures 7D and S6O).

Regulation of AMPK by SGK1 is conserved from mammals to *C. elegans* and governs whole organism starvation survival

Genes encoding components of the mTOR, AMPK, and PI3K pathways, including SGK, are well conserved from invertebrates to mammals. CeAMPK α ^{Thr243} (AAK-1/2, corresponding to human AMPK α ^{Thr172}) phosphorylation is elevated in *sgk-1* (the sole worm ortholog of mammalian SGK) mutant *C. elegans*, indicative of a conserved, inverse relationship between the activities of SGK and AMPK (Figure 7E). AMPK activity is essential for starvation survival and dietary restriction (DR)-induced lifespan extension in *C. elegans* (Greer and Brunet, 2009; Webster et al., 2017). Indeed, increased AMPK activity in *sgk-1* mutant *C. elegans* extends median (10%) and maximal (20%) survival under nutrient deprivation, an effect that is completely mitigated following RNAi to the AMPK α catalytic subunit *aak-2*. (Figure 7F).

DISCUSSION

Here, we report that liver-specific *Sgk1*-knockout mice demonstrate improvement in insulin sensitivity and protection against HFD-induced fatty liver. These favorable metabolic effects are mediated by loss of SGK1-mediated, inhibitory phosphorylation of AMPK α ^{Ser485/491}. Our data indicate that a major role of hepatic SGK1 is to negatively regulate insulin signaling by decreasing AMPK activity, resulting in a concomitant increase in mTORC1 activity. We suggest that this leads to increased negative feedback on insulin signaling, connecting SGK1 activation to promotion of hepatic insulin resistance. Our observation that SGK1 levels and activity are increased in the setting of insulin-resistant states further suggests that SGK1 directly links the PI3K-activated insulin signaling pathway to the development of insulin resistance. As expected, because loss of *Sgk1* drives metabolic change principally by increasing AMPK activity, it leads to decreased gluconeogenesis, decreased lipogenesis, and decreased body fat accumulation and ameliorates insulin resistance induced by HFD. Thus, *Sgk1* loss of function breaks the paradox in hepatic

insulin resistance, improving sensitivity to insulin-driven suppression of hepatic glucose output without increasing hepatic lipogenesis.

Regulation of systemic energy metabolism by SGK

A number of studies support our findings that SGK family kinases promote insulin resistance and obesity. The SGK1 inhibitor EMD638683 significantly decreases fasting blood glucose in *db/db* mice and diet-induced obesity in *Akt3*-knockout mice (Ding et al., 2017; Li et al., 2016). Conversely, transgenic expression of constitutively active SGK1 exacerbates diet-induced obesity and fatty liver (Sierra-Ramos et al., 2020). *Sgk1* mRNA is elevated in adipose tissue in obese mice and humans and is associated with inflammation (Li et al., 2013; Scherthaner-Reiter et al., 2015). Phosphorylation of SGK1^{Ser422} by mTORC2 is also increased in visceral fat of patients with T2D (Stafeev et al., 2019). A common (5%) polymorphism in human *SGK1* is associated with obesity and T2D (Dieter et al., 2004; Li et al., 2014; Schwab et al., 2008; von Wörm et al., 2005). In aggregate, these studies and data presented herein indicate that activation of SGK1 is mechanistically tied to the development of insulin resistance and obesity.

Our data suggest that of the SGK family members, SGK1 has the most prominent role in hepatic insulin action. Although knockdown of *SGK2* in human hepatocytes *ex vivo* has been shown to attenuate pregnane X receptor-regulated induction of *G6Pase* as well as glucose production (Gotoh and Negishi, 2014), here we show that *Sgk2*^{-/-} mice have very mild improvement in glucose tolerance that manifests only at a young age. *Sgk3* deficiency mitigates HFD-induced insulin resistance but not glucose intolerance. However, as glucose tolerance is reflective of insulin production and insulin action, the lack of difference in glucose tolerance in *Sgk3*^{-/-} mice could be due to the combined impact of a mild improvement in insulin sensitivity and a previously described defect in insulin secretion (Yao et al., 2011). As *Sgk* triple-knockout mice (*Sgk*^{Ltko}) do not demonstrate exaggerated insulin sensitivity, and primary hepatocytes from *Sgk1*^{-/-} and *Sgk*^{Ltko} demonstrate similar increases in insulin sensitivity, SGK1 is likely dominant among SGK family kinases in regulation of hepatic insulin action. Although unlikely to be evident in isolated hepatocytes, at the whole-animal level, it remains a distinct possibility that the global *Sgk2* and *Sgk3* knockouts used affect insulin sensitivity by action in other tissues. Definitive proof requires additional tissue-specific disruption of SGK kinases.

Our data conflict with data from a prior study demonstrating that SGK1 action increases insulin sensitivity in the liver by inhibiting ERK activity (Liu et al., 2014a). In this study, overexpression of *Sgk1* was shown to ameliorate insulin resistance in both glucosamine-treated HepG2 cells and livers of *db/db* mice. We cannot explain the discordance between our finding that *Sgk1*^{Lko} mice demonstrate increased insulin sensitivity versus this study demonstrating apparent insulin resistance. Our study uses the same *Sgk1* conditional mice and the same albumin-Cre as the study of Liu et al. (2014a). However, that study predominantly used short hairpin RNA (shRNA) knockdown to reduce SGK1 levels rather than their conditional *Sgk1* mice (Liu et al., 2014a). Importantly, consistent with our findings, Liu et al. (2014a) observed that SGK1 protein levels are higher in insulin-resistant *db/db* mice. We have confidence in the rigor of results presented here, given that multiple,

independent cohorts of mice, on multiple diets, and of both sexes demonstrate concordant findings. Differences in environment, such as those manifest as different microbiota, could contribute to discrepant data, and in fact this suggests compelling possibilities requiring further investigation. It is worth mentioning that SGK1 and Akt share an identical substrate recognition motif, and thus, as we and others have observed, overexpression of SGK1 can lead to non-physiological phosphorylation of Akt substrates including GSK3 α/β and FoxO3. As note of proof that these substrates represent predominantly Akt substrates, GSK3 α/β and FOXO3 phosphorylation levels are not changed in cells in which SGK1 cannot be activated (Collins et al., 2003). Finally, in support of findings presented here, BAC transgenic mice bearing the entire *Sgk1* gene with an activating point mutation develop obesity, glucose intolerance, and insulin resistance (Sierra-Ramos et al., 2020). In aggregate, our data and these observations support the notion that SGK1 antagonizes rather than facilitates insulin signaling.

Abnormal SGK1 accumulation promotes selective insulin resistance

Chronic overnutrition, including HFD feeding, causes hepatic-selective insulin resistance whereby there is resistance of the liver to the glucose-lowering properties of insulin but preservation of insulin-dependent lipogenesis (Petersen and Shulman, 2018). On the basis of work presented here, we hypothesize that SGK1 contributes mechanistically to selective insulin resistance by phosphorylating and inhibiting AMPK $\alpha^{\text{Ser485/491}}$. The decreased AMPK activity, along with a known activity of SGK1 to activate mTORC1 by phosphorylating and inhibiting TSC2 (Castel et al., 2016), (1) increases negative feedback on insulin signaling, (2) reduces hepatic lipid oxidation, and (3) promotes lipogenesis through SREBP-1c (Laplante and Sabatini, 2010), thereby facilitating selective insulin resistance. Our findings are in keeping with the previously reported ability of increased AMPK activity to decrease hepatic glucose production and lipid synthesis and increase fatty acid oxidation (Day et al., 2017). These data are also in agreement with prior work demonstrating that decreases in hepatic mTORC1 activity protects mice from Western diet-induced hepatic steatosis (Peterson et al., 2011). Although the exact mechanism by which mTORC1 negatively feeds back on insulin signaling remains a subject of some debate, the aggregate decreased serine phosphorylation of Irs1 and loss of Grb10 phosphorylation likely both contribute to increased insulin signaling in *Sgk1^{Lko}* mice (Copps et al., 2016; Harrington et al., 2004; Yu et al., 2011). Our results do not also rule out the distinct possibility that an additional means of improved insulin sensitivity in *Sgk1^{Lko}* mice is directly related to AMPK-dependent reduction in body fat mass, possibly exaggerated by parallel reductions in mTORC1 activity and lipogenesis. However, this is unlikely to be the sole mechanism, as improved insulin sensitivity is evident in *Sgk1^{Lko}* mice fed a chow diet, in which changes in hepatic lipid content and body fat mass are not evident. And finally, although not explicitly tested, it remains a distinct possibility that activation of hepatic AMPK in *Sgk1^{Lko}* mice facilitates glucose disposal by insulin-independent mechanisms, as has been demonstrated in skeletal muscle (O'Neill et al., 2011).

Our results draw a sharp distinction between the molecular function of two insulin- and mTORC2-activated protein kinases with identical substrate recognition motifs. Unlike knockout of hepatic *Akt* (Leavens et al., 2009), knockout of hepatic *Sgk1* selectively

improves insulin's ability to lower blood glucose without promoting HFD-induced hepatic steatosis. Accumulating evidence indicates that insulin signaling suppresses gluconeogenesis mainly by the mTORC2/AKT/FoxO pathway but activates lipogenesis through activation of AKT and SGK and subsequent parallel activation of mTORC1 and inhibition of FoxO (Haeusler et al., 2014; Titchenell et al., 2016; Wan et al., 2011). In the case of *Sgk1^{Lko}* mice, our data support at least two potential means by which insulin sensitivity is improved: (1) AMPK activation reduces fatty acid synthesis and enhances oxidation (evident at the level of gene expression and whole-body energy expenditure), and (2) inhibition of mTORC1 in *Sgk1^{Lko}* mice, as mTORC1 activity is necessary for stimulation of hepatic lipogenesis. We surmise that the concomitant enhanced activity of AMPK and reduced mTORC1 activity overcomes the increase in FoxO inhibition evident in *Sgk1^{Lko}* mice, protecting these animals from hepatic steatosis in the face of enhanced insulin signaling through Akt and FoxO.

Loss of hepatic SGK1 signaling mitigates selective hepatic insulin resistance through AMPK

AMPK is a central hub of metabolic regulation in liver, governing the balance of anabolic and catabolic metabolism of glucose and lipids. AMPK directly and indirectly reduces hepatic glucose production at the transcriptional level (Herzig and Shaw, 2018) and post-translationally by reducing mTORC1 activity reducing negative feedback on insulin signaling (Gwinn et al., 2008; Inoki et al., 2003). AMPK also increases fatty acid oxidation and decreases lipogenesis by phosphorylating and inhibiting ACC and HMG-CoA reductase, inhibiting transcription of lipogenic transcription factors ChREBP and SREBP, and by increasing mitochondrial biogenesis (Guigas et al., 2006; Herzig and Shaw, 2018; Woods et al., 2017).

These activities perfectly poise activation of hepatic AMPK to break the paradox in insulin resistance, an observation borne out by our data in *Sgk1^{Lko}* mice and in studies of AMPK. Broadly speaking, genetic or pharmacologic activation of AMPK reduces hepatic lipogenesis and reduces fatty liver disease, whereas genetic inactivation of AMPK promotes hyperglycemia and hepatic steatosis (Andreelli et al., 2006; Esquejo et al., 2018; Foretz et al., 2005; Garcia et al., 2019; Seo et al., 2009; Woods et al., 2017). However, there are paradoxes in data investigating the role of hepatic AMPK in insulin sensitivity. Although deletion of hepatic *Lkb1* in adult mice promotes marked hyperglycemia (Shaw et al., 2005), complete hepatic deficiency of AMPK α 1/2 does not appear to alter glucose homeostasis or insulin sensitivity (Viollet et al., 2009a). On the basis of our data, we suggest that in chowfed animals, impacts of SGK1 and AMPK on glucose homeostasis are subtle. Alternatively, in the setting of HFD consumption, augmented SGK1 signaling inhibiting AMPK clearly contributes to hyperglycemia, insulin resistance, weight gain, and hepatic steatosis. In aggregate, results from our studies and others imply that AMPK activity becomes particularly important during periods of nutrient excess.

It should be noted that overexpression of the active form of AMPK α 1^{Ser485Ala} does not completely recapitulate the effects of *Sgk1^{Lko}* mice in our experiments, particularly with regard to reduction in fat mass. It is possible that a duration of AMPK activation longer than that provided in our AAV-mediated experiments are necessary to reduce fat mass, for

example, that evident with near lifelong genetic deletion of *Sgk1*, or that SGK1 has effects beyond those on AMPK.

There is controversy on the precise role of AMPK α ^{S485/491} phosphorylation on AMPK activity. Early studies principally examined the AMPK α ^{S485/491} phosphorylation site for its role in full kinase activation, not inhibition; closer examination of those data indicate that phospho-mimic substitutions in AMPK α ^{S485} inhibit LKB1-mediated activation of AMPK by ~50% (Woods et al., 2003). In mouse embryonic fibroblasts (MEFs) and immortalized cells, AMPK α ^{S485} phosphorylation is reciprocally associated with AMPK activity, and AMPK α ^{S485A} substitution prevents inhibitory phosphorylation by cAMP-activated kinases (Hurley et al., 2006). In many instances the phosphorylation of AMPK α ^{S485} occurs concomitantly with AMPK α ^{T172} *in vivo* (Allen et al., 2017; Mount et al., 2012), but whether this is part of negative feedback on AMPK activity remains unclear. Adding to this uncertainty, certain data suggest that AMPK α ^{S485/S491} may be an AMPK autophosphorylation site (Hurley et al., 2006). We propose, on the basis of evidence presented here, that in the context of hepatocytes *in vivo*, SGK1-mediated phosphorylation of AMPK α ^{S485/491} represents an inhibitory input into AMPK, contributing to insulin resistance in animals fed a HFD.

Our observation that SGK1 activity increases in insulin resistance suggests that the kinase represents a significant component of the machinery contributing to selective insulin resistance in T2D. Our work indicates that SGK represents an answer to the elusive question of how insulin inhibits hepatic AMPK (via phosphorylation of AMPK α ^{Ser485/491}, which was postulated to be largely Akt independent) (Hardie, 2014; Hawley et al., 2014; Horman et al., 2006; Valentine et al., 2014). Loss of *Sgk1* may also activate AMPK through modulation of the mitochondrial permeability and energetics, but this requires further testing (Zhou et al., 2019). Our observations that AMPK α ^{Ser485Ala} expression *in vivo* improves hepatic insulin action and that this improvement phenocopies and is non-additive with hepatic *Sgk1* knockout suggest that a major role of SGK1 in hepatic metabolism is to negatively feed back on insulin signaling through AMPK. We propose that this activity can be selectively leveraged in order to break the paradox in insulin resistance present in T2D.

STAR*METHODS

RESOURCE AVAILABILITY

Lead contact—Further information and requests for resources and reagents should be directed to and will be fulfilled by the Lead Contact, Alexander A. Soukas (asoukas@mgh.harvard.edu).

Materials availability—Plasmids, cells, and mouse lines generated in this study will be made available upon request to the Lead Contact.

Data and code availability

- All data reported in this paper will be shared by the lead contact upon request.
- This study did not generate original code.

- Any additional information required to reanalyze the data reported in this paper is available from the lead contact upon request.

EXPERIMENTAL MODEL AND SUBJECT DETAILS

Mice—All mice were housed in a temperature-controlled room under a 12 hr light–dark cycle and under pathogen-free conditions. *Sgk1[flox/flox]* (RRID: MGI:5317851) mice were as we previously published (Fejes-Tóth et al., 2008). *Sgk1^{Lko}* mice were generated by crossing Albumin-Cre mice (The Jackson Laboratory, RRID: IMSR_JAX: 003574) with *Sgk1[flox/flox]* mice which were backcrossed with C57BL/6J mice for three times. Double *Sgk2;Sgk3* global knockout mice were generated by C57BL/6N zygotic injection of small guide RNAs targeting *Sgk2* and *Sgk3* and *S.p.Cas9* mRNA at the Genome Modification Facility, Harvard University. Mice were backcrossed four times prior to experimentation. *Sgk^{Ltko}* mice were generated by crossing *Sgk1^{Lko}* mice to *Sgk2;Sgk3* global knockout mice. Male mice were used to conduct most of the experiments except where indicated. Seminal experiments were repeated in both sexes. All animal procedures were approved under protocol 2010N000186 by Massachusetts General Hospital Subcommittee on Research Animal Care. Guide RNA sequences used are as follows:

Sgk2: CGGAGCCTTCTACGCCGTGA;

Sgk3: CAAGGCACTGGCGATCTCCG.

The age of mice used in each experiment can be found in Table S1.

Cell lines, culture conditions and transfection—AML12 hepatocytes (ATCC) were grown in a 1:1 mixture of DMEM and Ham's F12 medium (Thermo Fisher) with 0.005 mg/ml insulin, 0.005 mg/ml transferrin, 5 ng/ml selenium, 40 ng/ml dexamethasone, 10% fetal bovine serum (FBS, Sigma) and 1% penicillin-streptomycin (PS, Life Technologies), in a 5% CO₂ atmosphere at 37°C. Primary cultured mouse hepatocytes were prepared from C57BL/6J, liver-specific *Sgk1* knockout mice (genotype Albumin-*Cre*; *Sgk1[flox/flox]*) and their wild-type littermate controls (genotype *Sgk1[flox/flox]*) by collagenase perfusion method as described previously (Li et al., 2010), and were grown in Williams' Medium E supplemented with 10% FBS and 1% PS. HEK293T cells (ATCC) were grown in high glucose DMEM (Thermo Fisher) supplemented with 10% FBS and 1% PS in a 5% CO₂ atmosphere at 37°C. For transfection, Lipofectamine 3000 was used according to the instructions of manufacturer (Thermo Fisher). For Compound C treatment, cells were treated with vehicle or 5 μM Compound C for 18h and serum starved for 4h following insulin treatment.

METHOD DETAILS

Chemicals and antibodies—Compound C was obtained from Enzo Life Sciences. Sodium Palmitate is from NU-CHEK Prep Inc. For western blotting, anti-Flag M2 (RRID:AB_259529) antibody was purchased from Sigma, antibodies against SGK1 (RRID:AB_2687476), SGK2 (RRID:AB_10828732), SGK3 (RRID:AB_10949507), HSP90 (RRID:AB_2233307), Akt (RRID:AB_915783), p-Akt (Thr308) (RRID:AB_2255933), p-Akt (Ser473) (RRID:AB_2315049),

NDRG1 (RRID: AB_11140640), p-NDRG1(Thr346) (RRID:AB_10693451), FoxO1 (RRID:AB_2106495), p-FoxO1/3 (Thr24/32) (RRID:AB_2106814), S6K (RRID:AB_390722), p-S6K (Thr389) (RRID:AB_2269803), S6 (RRID:AB_331355), p-S6 (S240/244) (RRID:AB_10694233), 4EBP1 (RRID:AB_2097841), p-4EBP1 (Thr37/46) (RRID:AB_560835), p-4EBP1 (Ser65) (RRID:AB_330947), AMPK α (RRID:AB_10624867), p-AMPK α (Thr172) (RRID:AB_331250), p-AMPK α (Ser485/491) (RRID:AB_331250), ACC1 (RRID:AB_2219397), p-ACC1 (Ser79) (RRID:AB_330337), Raptor (RRID:AB_561245) and p-Raptor (Ser792) (RRID:AB_2249475) were obtained from Cell Signaling Technology. Anti-actin (C4) was obtained from Abcam.

Generation of Sgk1 knockout AML12 cells—*Sgk1* knockout AML12 cells were generated using CRISPR/Cas9 with modifications as described (Cong et al., 2013). Briefly, the px330 vector expressing Cas9 and guide RNA was electro-transfected into AML12 cells together with a plasmid conferring puromycin resistance. Forty-eight hours after transfection, puromycin was added to the cells at 5 μ g/ml for 48 hours, then puromycin resistant cells were trypsinized, counted and diluted to 10 cells/ml, then 100 μ L of the diluted cell mixture per well was seeded into a 96 well plate, and single-clones were expanded to generate stable cell lines. *Sgk1* knockout was confirmed by western blotting. Primers for sgRNA expression are: sense, 5'-CACCGTAAGCAGCCGTATGACCGGA-3', antisense, 5'-AAACTCCGGTCATACGGCTGCTTAC-3'.

Generation of recombinant adenoviruses and AAV—To construct adenoviruses expressing LacZ, AMPK α 2 and AMPK α 2-S491A, cDNAs encoding LacZ, AMPK α 2 and AMPK α 2-S491A were recombined into the pAd-CMV backbone, transfected into 293A cells, and purified to high titer with cesium chloride gradients. Adenovirus expressing constitutively activated SGK1 is a gift from Dr. Anthony Rosenzweig's lab at MGH. Primary hepatocytes were infected with adenovirus at M.O.I of 5 24h after plating the cells. To make AAV vectors expressing AMPK α 1^{Ser485Ala} and EGFP, three plasmids, pAd Delta F6, pAAV2/9 and pAAV.TBG.PI.eGFP.WPRE.bGH were purchased from the Penn vector core in University of Pennsylvania. cDNA encoding AMPK α 1^{Ser485Ala} was cloned in place of eGFP in pAAV.TBG.PI.eGFP.WPRE.bGH and virus packaging and high titer purification was done by Vigene Biosciences. Mice were injected 1×10^{11} purified viral particles per animal via tail vein, metabolic analysis were conducted at the indicated times.

Western blotting and co-immunoprecipitation—For western blotting, cell or tissue lysates were prepared in RIPA buffer (50 mM Tris-HCl pH 7.4, 150 mM NaCl, 1% Triton x-100, 1% Sodium deoxycholate, 0.1% SDS, 1 mM EDTA with 1x Complete protease inhibitor cocktail from Roche) unless otherwise indicated. Tissues were homogenized using a QIAGEN Tissue Lyser II. Lysates were cleared of insoluble material by centrifugation at 21,000g at 4°C and the supernatant was retained for western blotting. Protein concentration was determined using the Pierce BCA assay (Thermo Fisher). SDS-PAGE was conducted followed by electrophoretic transfer to nitrocellulose membrane at 100 V for 1 hour at 4°C. Immunoblots were performed according to primary antibody manufacturers' protocols. For immunodetection of primary antibodies, goat-anti-rabbit-HRP conjugate or goat-anti-mouse-HRP conjugate (GE Healthcare) was used at 1:5,000 in 5% BSA dissolved in TBST, and

HRP was detected using West-Pico chemiluminescence substrate (Thermo Pierce). The western blot results shown are representative of at least three independent experiments, and quantified results and statistics from biological replicates are shown wherever possible, as indicated in the figures and figure legends.

For the Co-IP assay, pCMV5-SGK1 and pcDNA3-AMPK α 1 were co-transfected into HEK293T cells. Mouse *Sgk1* was cloned into the pCMV5-Flag vector using the following primers:

Sgk1 forward, 5'- ATTTGCGGCCGCTGGAAGATGGTAAACAAAGACA -3',

Sgk1 reverse, 5'- TAGGATCCTCAGAGGAAGGAATCCACAGGA -3',

Forty-eight hours after transfection, cells were lysed using CHAPS lysis buffer (0.025 M Tris, 0.15 M NaCl, 0.5% CHAPS; pH 7.4), and lysate was incubated with anti-SGK1 antibody (Cell Signaling Technology) and protein A magnetic beads (New England Biolabs) following the manufacturer's protocol. Western blot was used for detection of AMPK α .

***In vitro* kinase assay**—To purify mouse SGK1 protein, Flag-SGK1 was transfected into HEK293T cells for 48h, cells were then lysed using RIPA buffer, and lysate was incubated with M2-Flag magnetic beads from SIGMA following its IP protocol. 3XFlag peptide was used to elute Flag-SGK1 from the beads. To purify AMPK α 1 protein, pcDNA3-AMPK α 1 with His tag was transfected into HEK293T cells for 48h and purified using the Pierce HisPur Ni-NTA Purification Kit (Thermo Scientific, Prod# 88227). SGK1(0.5 μ g) and AMPK α 1 (1 μ g) or AMPK α 2 β 1 γ 1 (1 μ g) complex were incubated in a 25ul reaction containing 5 μ L 5x kinase buffer, 1 mM DTT, and 500 μ M ATP for 15 min.

Quantitative RT-PCR—Worms and mouse tissues were flash frozen in liquid nitrogen and kept in -80°C until RNA preparation. To quantify changes in mRNA abundance in nematode and mammalian cells, total RNA was extracted using RNAzol RT (Molecular Research Center) according to manufacturer instructions. RNA was treated with RNase free DNase prior to reverse transcription with the Quantitect reverse transcription kit (QIAGEN). Quantitative RT-PCR was conducted in triplicate using a Quantitect SYBR Green PCR reagent (QIAGEN) following manufacturer instructions on a Bio-Rad CFX96 Real-Time PCR system (Bio-Rad) (see Key Resources Table for primer sequences). For mouse tissue samples, liver samples were homogenized in RNAzol using a TissueLyser II (QIAGEN), centrifuged for 10 min at 12,000 g to pellet debris, and the supernatant was collected and subjected to RNA extraction per the manufacturer protocol. Expression levels of tested genes were presented as normalized fold changes to the mRNA abundance of control genes indicated in the figures by the $\delta\delta\text{Ct}$ method.

Measurement of metabolic parameters—Mice were put on both standard chow diet (chow) (5008, Labdiets) or 60% kcal-fat high fat diet (HFD) (D12492, Research Diets) at weaning ~4 weeks of age. For glucose tolerance tests (GTT), mice were starved overnight (12 hours during the dark cycle) and I.P. injected with glucose at 2 g/kg body weight. For insulin tolerance test (ITT), mice were starved for 6h and I.P. injected at a concentration of 0.4 U/kg body weight of insulin for chow diet fed mice and 0.75 U/kg body weight for

HFD fed mice. MRI for body composition analysis was conducted at indicated times using an EchoMRI-100H, and energy expenditure was measured by indirect calorimetry using metabolic cages housed in environmental chambers (Sable Systems Promethion).

Biochemical and hormone assays—Glucose was measured with a glucometer specifically designed for mice (AlphaTrak2, Abbott Animal Health). Insulin, TG, total cholesterol, HDL, and ketones were measured according to manufacturer protocols (see Key Resource Table for suppliers). Tissue cholesterol and triglyceride contents were measured enzymatically following Folch extraction and lipid mass was normalized to tissue weight and protein content.

QUANTIFICATION AND STATISTICAL ANALYSIS

All western blotting quantifications were conducted in ImageJ. Statistical analyses were performed using Prism (GraphPad Software). The statistical differences between control and experimental groups were determined by two-tailed Student's *t* test (two groups), one-way ANOVA (more than two groups), two-way ANOVA (two independent experimental variables), or non-linear regression analysis as indicated in each figure legend, with numbers of samples indicated and corrected *p* values < 0.05 considered significant. Statistical details for each experiment can be found in each figure legend.

Supplementary Material

Refer to Web version on PubMed Central for supplementary material.

ACKNOWLEDGMENTS

We thank Joseph Avruch, Noriko Oshiro-Rapley, Ning Dai, and Laura Regue for discussions and reagents. Thanks to the Nutrition Obesity Research Center (NORC) at Harvard (P30DK040561) and the Boston Area Diabetes Endocrinology Research Center (DERC) (P30DK057521) for core services. This work was funded by NIH grants K08DK087941, R01DK101522, R56AG068999, and R01AG058256 (to A.A.S.), the Howard M. Goodman Fellowship (to A.A.S.), a Glenn Foundation Award for Research on the Biological Mechanisms of Aging (to A.A.S.), the Weissman Family Massachusetts General Hospital (MGH) Research Scholar Award (to A.A.S.), and an MGH Executive Committee on Research (ECOR) Postdoctoral Fellowship (to B.Z.).

REFERENCES

- Allen KM, Coughlan KA, Mahmood FN, Valentine RJ, Ruderman NB, and Saha AK (2017). The effects of troglitazone on AMPK in HepG2 cells. *Arch. Biochem. Biophys* 623–624, 49–57.
- Andreelli F, Foretz M, Knauf C, Cani PD, Perrin C, Iglesias MA, Pillot B, Bado A, Tronche F, Mithieux G, et al. (2006). Liver adenosine monophosphate-activated kinase- α 2 catalytic subunit is a key target for the control of hepatic glucose production by adiponectin and leptin but not insulin. *Endocrinology* 147, 2432–2441. [PubMed: 16455782]
- Bell P, Gao G, Haskins ME, Wang L, Sleeper M, Wang H, Calcedo R, Vandenberghe LH, Chen SJ, Weisse C, et al. (2011a). Evaluation of adeno-associated viral vectors for liver-directed gene transfer in dogs. *Hum. Gene Ther* 22, 985–997. [PubMed: 21204705]
- Bell P, Wang L, Gao G, Haskins ME, Tarantal AF, McCarter RJ, Zhu Y, Yu H, and Wilson JM (2011b). Inverse zonation of hepatocyte transduction with AAV vectors between mice and non-human primates. *Mol. Genet. Metab* 104, 395–403. [PubMed: 21778099]
- Böhmer C, Philippin M, Rajamanickam J, Mack A, Broer S, Palmada M, and Lang F (2004). Stimulation of the EAAT4 glutamate transporter by SGK protein kinase isoforms and PKB. *Biochem. Biophys. Res. Commun* 324, 1242–1248. [PubMed: 15504348]

- Brunet A, Park J, Tran H, Hu LS, Hemmings BA, and Greenberg ME (2001). Protein kinase SGK mediates survival signals by phosphorylating the forkhead transcription factor FKHL1 (FOXO3a). *Mol. Cell. Biol* 21, 952–965. [PubMed: 11154281]
- Castel P, Ellis H, Bago R, Toska E, Razavi P, Carmona FJ, Kannan S, Verma CS, Dickler M, Chandraratna S, et al. (2016). PDK1-SGK1 signaling sustains AKT-independent mTORC1 activation and confers resistance to PI3K α inhibition. *Cancer Cell* 30, 229–242. [PubMed: 27451907]
- Chen SJ, Sanmiguel J, Lock M, McMenamin D, Draper C, Limberis MP, Kassim SH, Somanathan S, Bell P, Johnston JC, et al. (2013). Biodistribution of AAV8 vectors expressing human low-density lipoprotein receptor in a mouse model of homozygous familial hypercholesterolemia. *Hum. Gene Ther. Clin. Dev* 24, 154–160. [PubMed: 24070336]
- Collins BJ, Deak M, Arthur JS, Armit LJ, and Alessi DR (2003). In vivo role of the PIF-binding docking site of PDK1 defined by knock-in mutation. *EMBO J.* 22, 4202–4211. [PubMed: 12912918]
- Cong L, Ran FA, Cox D, Lin S, Barretto R, Habib N, Hsu PD, Wu X, Jiang W, Marraffini LA, and Zhang F (2013). Multiplex genome engineering using CRISPR/Cas systems. *Science* 339, 819–823. [PubMed: 23287718]
- Copps KD, Hanç er NJ, Qiu W, and White MF (2016). Serine 302 phosphorylation of mouse insulin receptor substrate 1 (IRS1) is dispensable for normal insulin signaling and feedback regulation by hepatic S6 kinase. *J. Biol. Chem* 291, 8602–8617. [PubMed: 26846849]
- Czech MP (2017). Insulin action and resistance in obesity and type 2 diabetes. *Nat. Med* 23, 804–814. [PubMed: 28697184]
- Dagon Y, Hur E, Zheng B, Wellenstein K, Cantley LC, and Kahn BB (2012). p70S6 kinase phosphorylates AMPK on serine 491 to mediate leptin’s effect on food intake. *Cell Metab.* 16, 104–112. [PubMed: 22727014]
- Day EA, Ford RJ, and Steinberg GR (2017). AMPK as a therapeutic target for treating metabolic diseases. *Trends Endocrinol. Metab* 28, 545–560. [PubMed: 28647324]
- Dieter M, Palmada M, Rajamanickam J, Aydin A, Busjahn A, Boehmer C, Luft FC, and Lang F (2004). Regulation of glucose transporter SGLT1 by ubiquitin ligase Nedd4–2 and kinases SGK1, SGK3, and PKB. *Obes. Res* 12, 862–870. [PubMed: 15166308]
- Ding L, Zhang L, Biswas S, Schugar RC, Brown JM, Byzova T, and Podrez E (2017). Akt3 inhibits adipogenesis and protects from diet-induced obesity via WNK1/SGK1 signaling. *JCI Insight* 2, e95687.
- Djouder N, Tuerk RD, Suter M, Salvioni P, Thali RF, Scholz R, Vaahtomeri K, Auchli Y, Rechsteiner H, Brunisholz RA, et al. (2010). PKA phosphorylates and inactivates AMPK α to promote efficient lipolysis. *EMBO J.* 29, 469–481. [PubMed: 19942859]
- Esquejo RM, Salatto CT, Delmore J, Albuquerque B, Reyes A, Shi Y, Moccia R, Cokorinos E, Peloquin M, Monetti M, et al. (2018). Activation of liver AMPK with PF-06409577 corrects NAFLD and lowers cholesterol in rodent and primate preclinical models. *EBioMedicine* 31, 122–132. [PubMed: 29673898]
- Fejes-Tóth G, Frindt G, Náráy-Fejes-Tóth A, and Palmer LG (2008). Epithelial Na⁺ channel activation and processing in mice lacking SGK1. *Am. J. Physiol. Renal Physiol* 294, F1298–F1305. [PubMed: 18385268]
- Foretz M, Ancellin N, Andreelli F, Saintillan Y, Grondin P, Kahn A, Thorens B, Vaulont S, and Viollet B (2005). Short-term overexpression of a constitutively active form of AMP-activated protein kinase in the liver leads to mild hypoglycemia and fatty liver. *Diabetes* 54, 1331–1339. [PubMed: 15855317]
- Foretz M, Hébrard S, Leclerc J, Zarrinpashneh E, Soty M, Mithieux G, Sakamoto K, Andreelli F, and Viollet B (2010). Metformin inhibits hepatic gluconeogenesis in mice independently of the LKB1/AMPK pathway via a decrease in hepatic energy state. *J. Clin. Invest* 120, 2355–2369. [PubMed: 20577053]
- Garcia D, Hellberg K, Chaix A, Wallace M, Herzig S, Badur MG, Lin T, Shokhirev MN, Pinto AFM, Ross DS, et al. (2019). Genetic liver-specific AMPK activation protects against diet-induced obesity and NAFLD. *Cell Rep.* 26, 192–208.e6. [PubMed: 30605676]

- García-Martínez JM, and Alessi DR (2008). mTOR complex 2 (mTORC2) controls hydrophobic motif phosphorylation and activation of serum- and glucocorticoid-induced protein kinase 1 (SGK1). *Biochem. J* 416, 375–385. [PubMed: 18925875]
- Gotoh S, and Negishi M (2014). Serum- and glucocorticoid-regulated kinase 2 determines drug-activated pregnane X receptor to induce gluconeogenesis in human liver cells. *J. Pharmacol. Exp. Ther* 348, 131–140. [PubMed: 24204015]
- Greer EL, and Brunet A (2009). Different dietary restriction regimens extend lifespan by both independent and overlapping genetic pathways in *C. elegans*. *Aging Cell* 8, 113–127. [PubMed: 19239417]
- Guigas B, Bertrand L, Taleux N, Foretz M, Wiernsperger N, Vertommen D, Andreelli F, Viollet B, and Hue L (2006). 5-Aminoimidazole-4-carboxamide-1-beta-D-ribofuranoside and metformin inhibit hepatic glucose phosphorylation by an AMP-activated protein kinase-independent effect on glucokinase translocation. *Diabetes* 55, 865–874. [PubMed: 16567505]
- Guo S (2014). Insulin signaling, resistance, and the metabolic syndrome: insights from mouse models into disease mechanisms. *J. Endocrinol* 220, T1–T23. [PubMed: 24281010]
- Gwinn DM, Shackelford DB, Egan DF, Mihaylova MM, Mery A, Vasquez DS, Turk BE, and Shaw RJ (2008). AMPK phosphorylation of raptor mediates a metabolic checkpoint. *Mol. Cell* 30, 214–226. [PubMed: 18439900]
- Haeusler RA, Hartil K, Vaitheesvaran B, Arrieta-Cruz I, Knight CM, Cook JR, Kammoun HL, Febbraio MA, Gutierrez-Juarez R, Kurland IJ, and Accili D (2014). Integrated control of hepatic lipogenesis versus glucose production requires FoxO transcription factors. *Nat. Commun* 5, 5190. [PubMed: 25307742]
- Hagiwara A, Cornu M, Cybulski N, Polak P, Betz C, Trapani F, Terracciano L, Heim MH, Rüegg MA, and Hall MN (2012). Hepatic mTORC2 activates glycolysis and lipogenesis through Akt, glucokinase, and SREBP1c. *Cell Metab.* 15, 725–738. [PubMed: 22521878]
- Hardie DG (2003). Minireview: the AMP-activated protein kinase cascade: the key sensor of cellular energy status. *Endocrinology* 144, 5179–5183. [PubMed: 12960015]
- Hardie DG (2014). AMPK—sensing energy while talking to other signaling pathways. *Cell Metab.* 20, 939–952. [PubMed: 25448702]
- Harrington LS, Findlay GM, Gray A, Tolkacheva T, Wigfield S, Rebholz H, Barnett J, Leslie NR, Cheng S, Shepherd PR, et al. (2004). The TSC1–2 tumor suppressor controls insulin-PI3K signaling via regulation of IRS proteins. *J. Cell Biol* 166, 213–223. [PubMed: 15249583]
- Haruta T, Uno T, Kawahara J, Takano A, Egawa K, Sharma PM, Olefsky JM, and Kobayashi M (2000). A rapamycin-sensitive pathway down-regulates insulin signaling via phosphorylation and proteasomal degradation of insulin receptor substrate-1. *Mol. Endocrinol* 14, 783–794. [PubMed: 10847581]
- Hawley SA, Ross FA, Gowans GJ, Tibarewal P, Leslie NR, and Hardie DG (2014). Phosphorylation by Akt within the ST loop of AMPK- α 1 down-regulates its activation in tumour cells. *Biochem. J* 459, 275–287. [PubMed: 24467442]
- Herzig S, and Shaw RJ (2018). AMPK: guardian of metabolism and mitochondrial homeostasis. *Nat. Rev. Mol. Cell Biol.* 19, 121–135. [PubMed: 28974774]
- Horman S, Vertommen D, Heath R, Neumann D, Mouton V, Woods A, Schlattner U, Wallimann T, Carling D, Hue L, and Rider MH (2006). Insulin antagonizes ischemia-induced Thr172 phosphorylation of AMP-activated protein kinase alpha-subunits in heart via hierarchical phosphorylation of Ser485/491. *J. Biol. Chem* 281, 5335–5340. [PubMed: 16340011]
- Hsu PP, Kang SA, Rameseder J, Zhang Y, Ottina KA, Lim D, Peterson TR, Choi Y, Gray NS, Yaffe MB, et al. (2011). The mTOR-regulated phosphoproteome reveals a mechanism of mTORC1-mediated inhibition of growth factor signaling. *Science* 332, 1317–1322. [PubMed: 21659604]
- Hurley RL, Barré LK, Wood SD, Anderson KA, Kemp BE, Means AR, and Witters LA (2006). Regulation of AMP-activated protein kinase by multisite phosphorylation in response to agents that elevate cellular cAMP. *J. Biol. Chem* 281, 36662–36672. [PubMed: 17023420]
- Inoki K, Zhu T, and Guan KL (2003). TSC2 mediates cellular energy response to control cell growth and survival. *Cell* 115, 577–590. [PubMed: 14651849]

- Jiang P, Ren L, Zhi L, Yu Z, Lv F, Xu F, Peng W, Bai X, Cheng K, Quan L, et al. (2021). Negative regulation of AMPK signaling by high glucose via E3 ubiquitin ligase MG53. *Mol. Cell* 81, 629–637.e5. [PubMed: 33400924]
- Khamzina L, Veilleux A, Bergeron S, and Marette A (2005). Increased activation of the mammalian target of rapamycin pathway in liver and skeletal muscle of obese rats: possible involvement in obesity-linked insulin resistance. *Endocrinology* 146, 1473–1481. [PubMed: 15604215]
- Kobayashi T, Deak M, Morrice N, and Cohen P (1999). Characterization of the structure and regulation of two novel isoforms of serum- and glucocorticoid-induced protein kinase. *Biochem. J* 344, 189–197. [PubMed: 10548550]
- Lamming DW, Ye L, Katajisto P, Goncalves MD, Saitoh M, Stevens DM, Davis JG, Salmon AB, Richardson A, Ahima RS, et al. (2012). Rapamycin-induced insulin resistance is mediated by mTORC2 loss and uncoupled from longevity. *Science* 335, 1638–1643. [PubMed: 22461615]
- Laplante M, and Sabatini DM (2010). mTORC1 activates SREBP-1c and uncouples lipogenesis from gluconeogenesis. *Proc. Natl. Acad. Sci. USA* 107, 3281–3282. [PubMed: 20167806]
- Leavens KF, Easton RM, Shulman GI, Previs SF, and Birnbaum MJ (2009). Akt2 is required for hepatic lipid accumulation in models of insulin resistance. *Cell Metab.* 10, 405–418. [PubMed: 19883618]
- Li WC, Ralphs KL, and Tosh D (2010). Isolation and culture of adult mouse hepatocytes. *Methods Mol. Biol* 633, 185–196. [PubMed: 20204628]
- Li P, Pan F, Hao Y, Feng W, Song H, and Zhu D (2013). SGK1 is regulated by metabolic-related factors in 3T3-L1 adipocytes and overexpressed in the adipose tissue of subjects with obesity and diabetes. *Diabetes Res. Clin. Pract* 102, 35–42. [PubMed: 24035040]
- Li C, Yang X, He J, Hixson JE, Gu D, Rao DC, Shimmin LC, Huang J, Gu CC, Chen J, et al. (2014). A gene-based analysis of variants in the serum/glucocorticoid regulated kinase (SGK) genes with blood pressure responses to sodium intake: the GenSalt Study. *PLoS ONE* 9, e98432. [PubMed: 24878720]
- Li P, Hao Y, Pan FH, Zhang M, Ma JQ, and Zhu DL (2016). SGK1 inhibitor reverses hyperglycemia partly through decreasing glucose absorption. *J. Mol. Endocrinol.* 56, 301–309. [PubMed: 27287220]
- Liu H, Yu J, Xia T, Xiao Y, Zhang Q, Liu B, Guo Y, Deng J, Deng Y, Chen S, et al. (2014a). Hepatic serum- and glucocorticoid-regulated protein kinase 1 (SGK1) regulates insulin sensitivity in mice via extracellular-signalregulated kinase 1/2 (ERK1/2). *Biochem. J* 464, 281–289. [PubMed: 25222560]
- Liu X, Chhipa RR, Nakano I, and Dasgupta B (2014b). The AMPK inhibitor compound C is a potent AMPK-independent antiangioma agent. *Mol. Cancer Ther* 13, 596–605. [PubMed: 24419061]
- Liu P, Gan W, Chin YR, Ogura K, Guo J, Zhang J, Wang B, Blenis J, Cantley LC, Toker A, et al. (2015). PtdIns(3,4,5)P3-Dependent Activation of the mTORC2 Kinase Complex. *Cancer Discov.* 5, 1194–1209. [PubMed: 26293922]
- Mount PF, Gleich K, Tam S, Fraser SA, Choy SW, Dwyer KM, Lu B, Denderen BV, Fingerle-Rowson G, Bucala R, et al. (2012). The outcome of renal ischemia-reperfusion injury is unchanged in AMPK- β 1 deficient mice. *PLoS ONE* 7, e29887. [PubMed: 22253816]
- O’Neill HM, Maarbjerg SJ, Crane JD, Jeppesen J, Jørgensen SB, Schertzer JD, Shyroka O, Kiens B, van Denderen BJ, Tarnopolsky MA, et al. (2011). AMP-activated protein kinase (AMPK) β 1 β 2 muscle null mice reveal an essential role for AMPK in maintaining mitochondrial content and glucose uptake during exercise. *Proc. Natl. Acad. Sci. U S A* 108, 16092–16097. [PubMed: 21896769]
- Petersen MC, and Shulman GI (2018). Mechanisms of insulin action and insulin resistance. *Physiol. Rev* 98, 2133–2223. [PubMed: 30067154]
- Peterson TR, Sengupta SS, Harris TE, Carmack AE, Kang SA, Balderas E, Guertin DA, Madden KL, Carpenter AE, Finck BN, and Sabatini DM (2011). mTOR complex 1 regulates lipin 1 localization to control the SREBP pathway. *Cell* 146, 408–420. [PubMed: 21816276]
- Rondinone CM (2007). Kinase-dependent pathways and the development of insulin resistance in hepatocytes. *Expert Rev. Endocrinol. Metab.* 2, 195–203. [PubMed: 30754170]

- Ruddock MW, Stein A, Landaker E, Park J, Cooksey RC, McClain D, and Patti ME (2008). Saturated fatty acids inhibit hepatic insulin action by modulating insulin receptor expression and post-receptor signalling. *J. Biochem* 144, 599–607. [PubMed: 18713797]
- Samuel VT, Liu ZX, Qu X, Elder BD, Bilz S, Befroy D, Romanelli AJ, and Shulman GI (2004). Mechanism of hepatic insulin resistance in non-alcoholic fatty liver disease. *J. Biol. Chem* 279, 32345–32353. [PubMed: 15166226]
- Sarbassov DD, Guertin DA, Ali SM, and Sabatini DM (2005). Phosphorylation and regulation of Akt/PKB by the rictor-mTOR complex. *Science* 307, 1098–1101. [PubMed: 15718470]
- Scherthamer-Reiter MH, Kiefer F, Zeyda M, Stulnig TM, Luger A, and Vila G (2015). Strong association of serum- and glucocorticoid-regulated kinase 1 with peripheral and adipose tissue inflammation in obesity. *Int. J. Obes* 39, 1143–1150.
- Schwab M, Lupescu A, Mota M, Mota E, Frey A, Simon P, Mertens PR, Floege J, Luft F, Asante-Poku S, et al. (2008). Association of SGK1 gene polymorphisms with type 2 diabetes. *Cell. Physiol. Biochem* 21, 151–160. [PubMed: 18209482]
- Seo E, Park EJ, Joe Y, Kang S, Kim MS, Hong SH, Park MK, Kim DK, Koh H, and Lee HJ (2009). Overexpression of AMPK α 1 ameliorates fatty liver in hyperlipidemic diabetic rats. *Korean J. Physiol. Pharmacol* 13, 449–454. [PubMed: 20054491]
- Shaw RJ, Lamia KA, Vasquez D, Koo SH, Bardeesy N, Depinho RA, Montminy M, and Cantley LC (2005). The kinase LKB1 mediates glucose homeostasis in liver and therapeutic effects of metformin. *Science* 310, 1642–1646. [PubMed: 16308421]
- Sierra-Ramos C, Velazquez-Garcia S, Vastola-Mascolo A, Hernández G, Faresse N, and Alvarez de la Rosa D (2020). SGK1 activation exacerbates diet-induced obesity, metabolic syndrome and hypertension. *J. Endocrinol* 244, 149–162. [PubMed: 31600722]
- Sommer EM, Dry H, Cross D, Guichard S, Davies BR, and Alessi DR (2013). Elevated SGK1 predicts resistance of breast cancer cells to Akt inhibitors. *Biochem. J* 452, 499–508. [PubMed: 23581296]
- Stafeev IS, Sklyanik IA, Yah'yaev KA, Shestakova EA, Yurasov AV, Karmadonov AV, Chibalin AV, Yu Menshikov M, Vorotnikov AV, Parfyonova YV, and Shestakova MV (2019). Low AS160 and high SGK basal phosphorylation associates with impaired incretin profile and type 2 diabetes in adipose tissue of obese patients. *Diabetes Res. Clin. Pract* 158, 107928. [PubMed: 31734225]
- Titchenell PM, Quinn WJ, Lu M, Chu Q, Lu W, Li C, Chen H, Monks BR, Chen J, Rabinowitz JD, and Birnbaum MJ (2016). Direct hepatocyte insulin signaling is required for lipogenesis but is dispensable for the suppression of glucose production. *Cell Metab.* 23, 1154–1166. [PubMed: 27238637]
- Unger RH, and Zhou YT (2001). Lipotoxicity of beta-cells in obesity and in other causes of fatty acid spillover. *Diabetes* 50 (Suppl 1), S118–S121. [PubMed: 11272168]
- Valentine RJ, Coughlan KA, Ruderman NB, and Saha AK (2014). Insulin inhibits AMPK activity and phosphorylates AMPK Ser485/491 through Akt in hepatocytes, myotubes and incubated rat skeletal muscle. *Arch. Biochem. Biophys* 562, 62–69. [PubMed: 25172224]
- Viana AY, Sakoda H, Anai M, Fujishiro M, Ono H, Kushiyaama A, Fukushima Y, Sato Y, Oshida Y, Uchijima Y, et al. (2006). Role of hepatic AMPK activation in glucose metabolism and dexamethasone-induced regulation of AMPK expression. *Diabetes Res. Clin. Pract* 73, 135–142. [PubMed: 16503364]
- Viollet B, Athea Y, Mounier R, Guigas B, Zarrinpashneh E, Horman S, Lantier L, Hebrard S, Devin-Leclerc J, Beauloye C, et al. (2009a). AMPK: lessons from transgenic and knockout animals. *Front. Biosci* 14, 19–44.
- Viollet B, Guigas B, Leclerc J, Hébrard S, Lantier L, Mounier R, Andreelli F, and Foretz M (2009b). AMP-activated protein kinase in the regulation of hepatic energy metabolism: from physiology to therapeutic perspectives. *Acta Physiol. (Oxf.)* 196, 81–98. [PubMed: 19245656]
- von Wowern F, Berglund G, Carlson J, Månsson H, Hedblad B, and Melander O (2005). Genetic variance of SGK-1 is associated with blood pressure, blood pressure change over time and strength of the insulin-diastolic blood pressure relationship. *Kidney Int.* 68, 2164–2172. [PubMed: 16221215]
- Wan M, Leavens KF, Saleh D, Easton RM, Guertin DA, Peterson TR, Kaestner KH, Sabatini DM, and Birnbaum MJ (2011). Postprandial hepatic lipid metabolism requires signaling through Akt2

- independent of the transcription factors FoxA2, FoxO1, and SREBP1c. *Cell Metab.* 14, 516–527. [PubMed: 21982711]
- Webster CM, Pino EC, Carr CE, Wu L, Zhou B, Cedillo L, Kacergis MC, Curran SP, and Soukas AA (2017). Genome-wide RNAi screen for fat regulatory genes in *C. elegans* identifies a proteostasis-AMPK axis critical for starvation survival. *Cell Rep.* 20, 627–640. [PubMed: 28723566]
- Witters LA, and Kemp BE (1992). Insulin activation of acetyl-CoA carboxylase accompanied by inhibition of the 5'-AMP-activated protein kinase. *J. Biol. Chem.* 267, 2864–2867. [PubMed: 1346611]
- Woods A, Vertommen D, Neumann D, Turk R, Bayliss J, Schlattner U, Wallimann T, Carling D, and Rider MH (2003). Identification of phosphorylation sites in AMP-activated protein kinase (AMPK) for upstream AMPK kinases and study of their roles by site-directed mutagenesis. *J. Biol. Chem.* 278, 28434–28442. [PubMed: 12764152]
- Woods A, Williams JR, Muckett PJ, Mayer FV, Liljevald M, Bohlooly-Y M, and Carling D (2017). Liver-specific activation of AMPK prevents steatosis on a high-fructose diet. *Cell Rep.* 18, 3043–3051. [PubMed: 28355557]
- Yan Z, Yan H, and Ou H (2012). Human thyroxine binding globulin (TBG) promoter directs efficient and sustaining transgene expression in liver-specific pattern. *Gene* 506, 289–294. [PubMed: 22820390]
- Yang J, Maika S, Craddock L, King JA, and Liu ZM (2008). Chronic activation of AMP-activated protein kinase- α 1 in liver leads to decreased adiposity in mice. *Biochem. Biophys. Res. Commun* 370, 248–253. [PubMed: 18381066]
- Yao LJ, McCormick JA, Wang J, Yang KY, Kidwai A, Colussi GL, Boini KM, Birnbaum MJ, Lang F, German MS, and Pearce D (2011). Novel role for SGK3 in glucose homeostasis revealed in SGK3/Akt2 double null mice. *Mol. Endocrinol* 25, 2106–2118. [PubMed: 21980074]
- Yu Y, Yoon SO, Poulogiannis G, Yang Q, Ma XM, Villén J, Kubica N, Hoffman GR, Cantley LC, Gygi SP, and Blenis J (2011). Phosphoproteomic analysis identifies Grb10 as an mTORC1 substrate that negatively regulates insulin signaling. *Science* 332, 1322–1326. [PubMed: 21659605]
- Yuan M, Pino E, Wu L, Kacergis M, and Soukas AA (2012). Identification of Akt-independent regulation of hepatic lipogenesis by mammalian target of rapamycin (mTOR) complex 2. *J. Biol. Chem* 287, 29579–29588. [PubMed: 22773877]
- Zhao P, Sun X, Chagga C, Liao Z, In Wong K, He F, Singh S, Loomba R, Karin M, Witztum JL, and Saltiel AR (2020). An AMPK-caspase-6 axis controls liver damage in nonalcoholic steatohepatitis. *Science* 367, 652–660. [PubMed: 32029622]
- Zhou B, Kreuzer J, Kumsta C, Wu L, Kamber KJ, Cedillo L, Zhang Y, Li S, Kacergis MC, Webster CM, et al. (2019). Mitochondrial permeability uncouples elevated autophagy and lifespan extension. *Cell* 177, 299–314.e16. [PubMed: 30929899]

Highlights

- SGK1 drives insulin resistance in liver in response to high-fat diet consumption
- SGK1 promotes insulin resistance by phosphorylating and inhibiting AMPK
- Expression of AMPK that cannot be acted upon by SGK1 promotes insulin sensitivity
- SGK1 is dominant among SGK family kinases regulating insulin sensitivity in liver

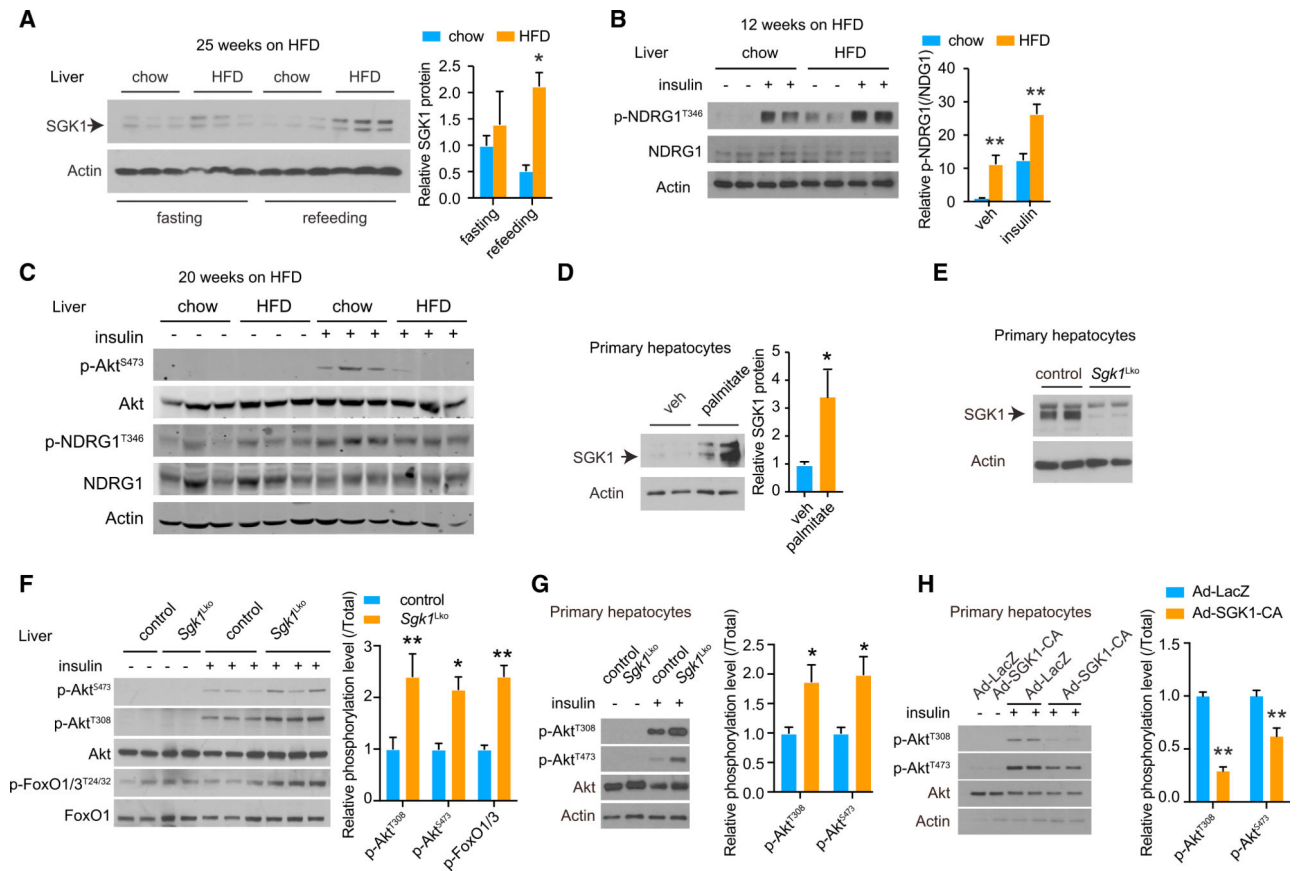


Figure 1. SGK1 action inhibits insulin-Akt-FoxO signaling

(A) SGK1 western blot under fasting and refeeding conditions (left panel). Liver tissue from normal diet (chow) and HFD fed mice fasted for 16 h or fed for 2 h after 16 h fasting. Relative protein levels are quantitated in the right panel (n = 3 male mice per group).

(B) NDRG1 phosphorylation in chow versus HFD mouse liver 15 min following injection of vehicle or 2 U/kg insulin after 16 h fasting by blot (left panel) and quantitated (right panel; n = 4 male mice per group).

(C) Phosphorylation of Akt^{S473} is attenuated whereas NDRG1^{T346} is preserved following 20 weeks of HFD feeding (n = 3 wild-type male mice per group).

(D) SGK1 protein level in mouse primary hepatocytes following 250 μM palmitate treatment for 18 h (left panel), quantitated in the right panel (n = 4 biological replicates per group).

(E) Knockout of hepatic *Sgk1* confirmed by western blot.

(F) Phosphorylation of Akt and FoxO by western blot 15 min after insulin injection (2 U/kg) in wild-type and *Sgk1*^{Lko} liver, quantitated on the right panel (n = 3 per group).

(G) Phosphorylation of Akt^{Thr308/Ser473} by western blot in primary cultured mouse hepatocytes after serum starvation for 4 h followed by vehicle or insulin (50 nM) treatment for 15 min, quantitated in the right panel (n = 3 biological replicates per group).

(H) Adenovirus-mediated overexpression of constitutively activated SGK1^{Ser422Asp} (SGK1-CA) in primary cultured hepatocytes decreases Akt^{Ser473} and Akt^{Thr308} phosphorylation levels following insulin treatment. Cells were serum starved for 4 h and treated with insulin (50 nM) for 15 min, quantitated in the right panel (n = 3 biological replicates per group).

See also Figure S1 and Table S1 for information on mouse sex, age, n, and replication. * $p < 0.05$ and ** $p < 0.01$ by two-way ANOVA (A, B, and F–H) or by t test (D). All bars indicate mean and SEM.

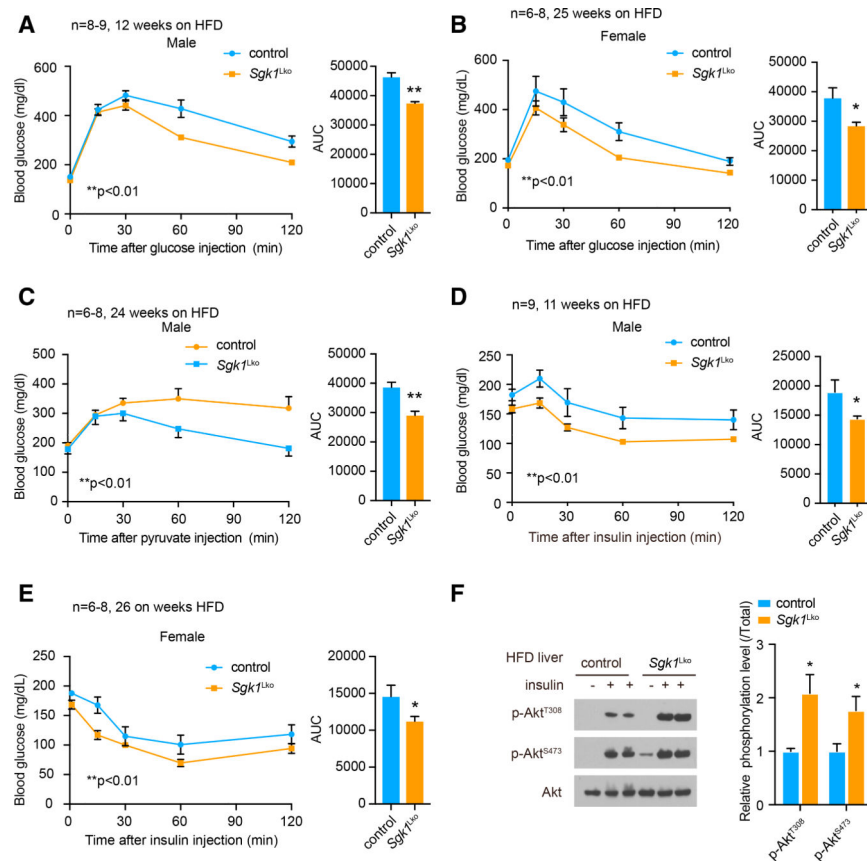


Figure 2. *Sgk1*^{Lko} mice manifest improved glucose homeostasis when fed a high-fat diet (HFD) (A and B) I.p. glucose tolerance tests (1 g/kg) in male control (*Sgk1*[flox/flox]) (n = 8) and *Sgk1*^{Lko} mice (n = 9) fed a HFD for 12 weeks (A) and female control (n = 6) and *Sgk1*^{Lko} mice (n = 8) fed a HFD for 25 weeks (B). AUC, area under the curve.

(C) I.p. pyruvate tolerance tests (2 g/kg) in male control (n = 6) and *Sgk1*^{Lko} mice (n = 8) fed a HFD for 24 weeks.

(D and E) I.p. insulin tolerance tests (0.4 U/kg) in male control (n = 8) and *Sgk1*^{Lko} mice (n = 8) fed a HFD for 11 weeks (D) and female control (n = 6) and *Sgk1*^{Lko} mice (n = 8) fed a HFD for 26 weeks (E).

(F) Phosphorylation of Akt in liver assessed by western blot 15 min after insulin injection (5 U/kg) in control and *Sgk1*^{Lko} mice fed HFD for 16 weeks, quantitated in the right panel (n = 4 per group).

See also Figure S2 and Table S1 for information on n and replication. *p < 0.05 and **p < 0.01 by t test (A–E; AUC), by two-way ANOVA (A–E; p value indicated on graph for control versus *Sgk1*^{Lko}), or by two-way ANOVA (F). All bars indicate mean and SEM.

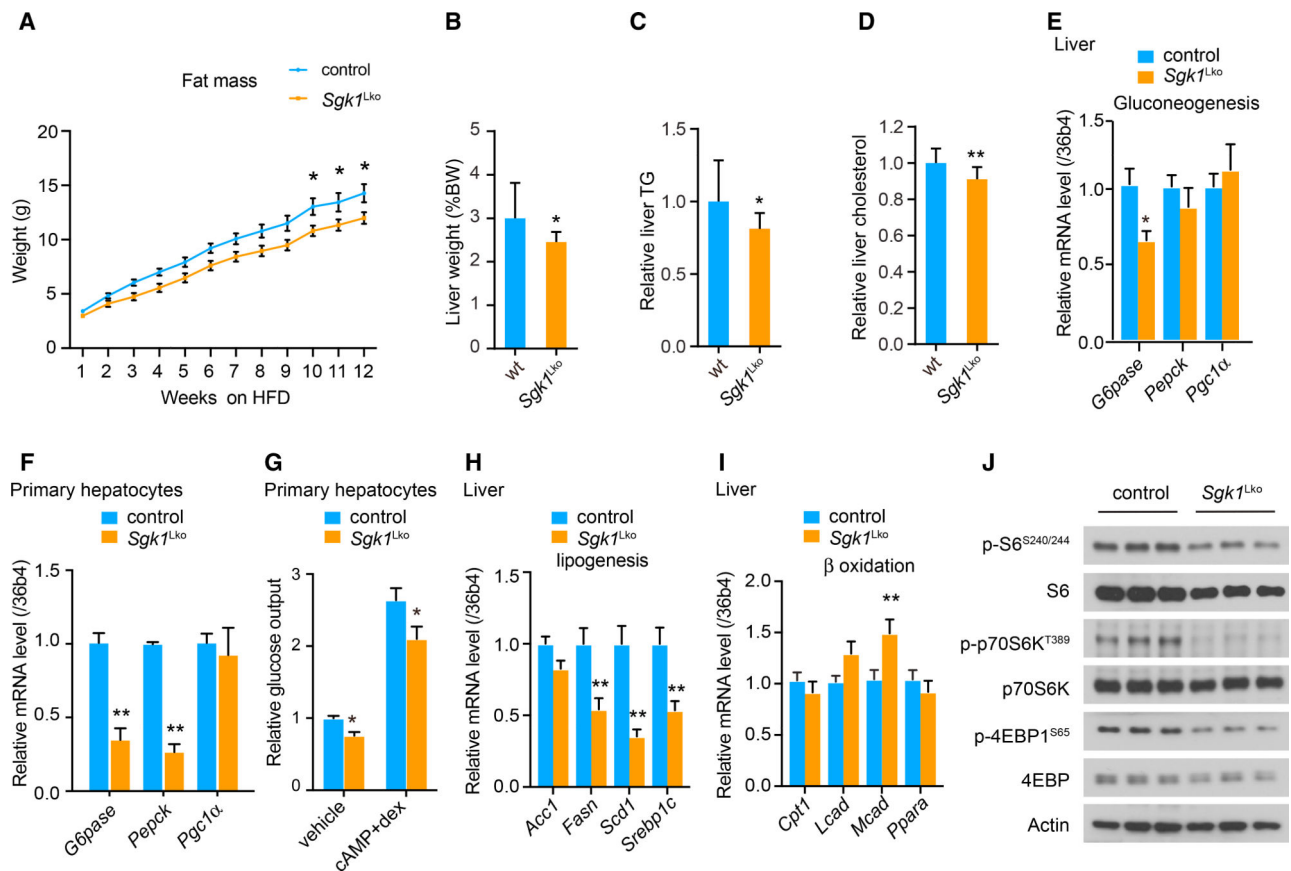


Figure 3. Hepatic knockout of *Sgk1* protects mice from HFD-induced weight gain, fatty liver, and glucose intolerance

(A) Fat mass of control (n = 23) and *Sgk1*^{Lko} (n = 23) mice fed a HFD.

(B–D) Liver weight (B), liver triglyceride (C), and liver cholesterol levels (D) from control (n = 12) and *Sgk1*^{Lko} (n = 13) mice fed a HFD for 16 weeks and starved for 12 h overnight.

(E) Hepatic gluconeogenic gene mRNA levels in control (n = 7) and *Sgk1*^{Lko} mice (n = 5) fed with HFD for 16 weeks and starved for 12 h overnight.

(F) mRNA levels of gluconeogenesis genes in control versus *Sgk1*^{Lko} primary hepatocytes (n = 5 biological replicates per group).

(G) Glucose production under basal and cAMP/dexamethasone (dex) treatment conditions in control versus *Sgk1*^{Lko} primary hepatocytes (n = 9 biological replicates per group).

(H and I) Hepatic lipogenesis and fatty acid oxidation gene mRNA levels in control (n = 12) and *Sgk1*^{Lko} (n = 8) male mice. Mice were fed with HFD for 16 weeks and starved for 12 h overnight prior to collecting liver tissue.

(J) Decreased mTORC1 target phosphorylation in livers of *Sgk1*^{Lko} mice as evident by decreased phospho-p70S6K^{Thr389} and phospho-4EBP1^{Ser65/Thr37/46}.

See also Figure S3 and Table S1 for information on mouse sex, age, n, and replication. *p < 0.05 and **p < 0.01 by two-way ANOVA (A, E, F, and H) or t test (B–D and G). All bars indicate mean and SEM.

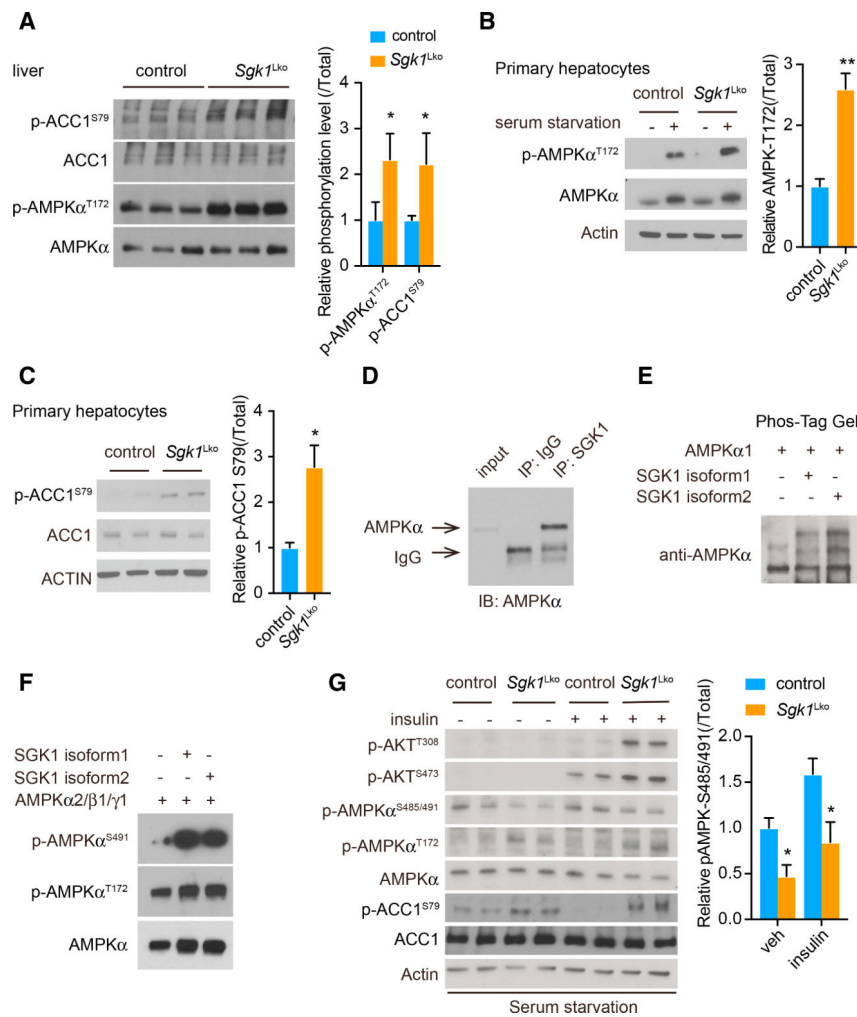


Figure 4. SGK1 directly inhibits AMPK activity by phosphorylating AMPKα^{Ser485/491}
 (A) Phosphorylation of AMPKα^{Thr172} and ACC1^{Ser79} in liver following starvation for 16 h overnight, quantitated in the right panel (n = 3 male mice per group).
 (B) AMPKα^{Thr172} phosphorylation in *Sgk1*-knockout versus control hepatocytes under serum starvation, quantitated in the right panel (n = 5 biological replicates per group).
 (C) Phosphorylation of ACC1^{Ser79} in mouse primary cultured hepatocytes, quantitated in the right panel (n = 3 biological replicates per group).
 (D) AMPKα co-immunoprecipitates with SGK1 (versus IgG negative control).
 (E) SGK1 phosphorylates AMPKα *in vitro*, as revealed by retarded mobility on a Phos-Tag gel. Two immunopurified SGK1 isoforms phosphorylate AMPKα.
 (F) Phosphorylation of AMPKα^{Ser491} following incubation of recombinant AMPKα2/β1/γ1 with either of two isoforms of SGK1 *in vitro*.
 (G) Phosphorylation of AMPKα^{Ser485/491} is reduced in *Sgk1*-knockout hepatocytes under basal and insulin-stimulated conditions, quantitated in the right panel (n = 4 biological replicates per group), with a parallel increase in AMPK activity, evidenced by increased phospho-ACC^{S79}

See also Figure S4 and Table S1 for information on mouse sex, age, n, and replication. * $p < 0.05$ and ** $p < 0.01$ by two-way ANOVA (A and G) and t test (B and C). All bars indicate mean and SEM.

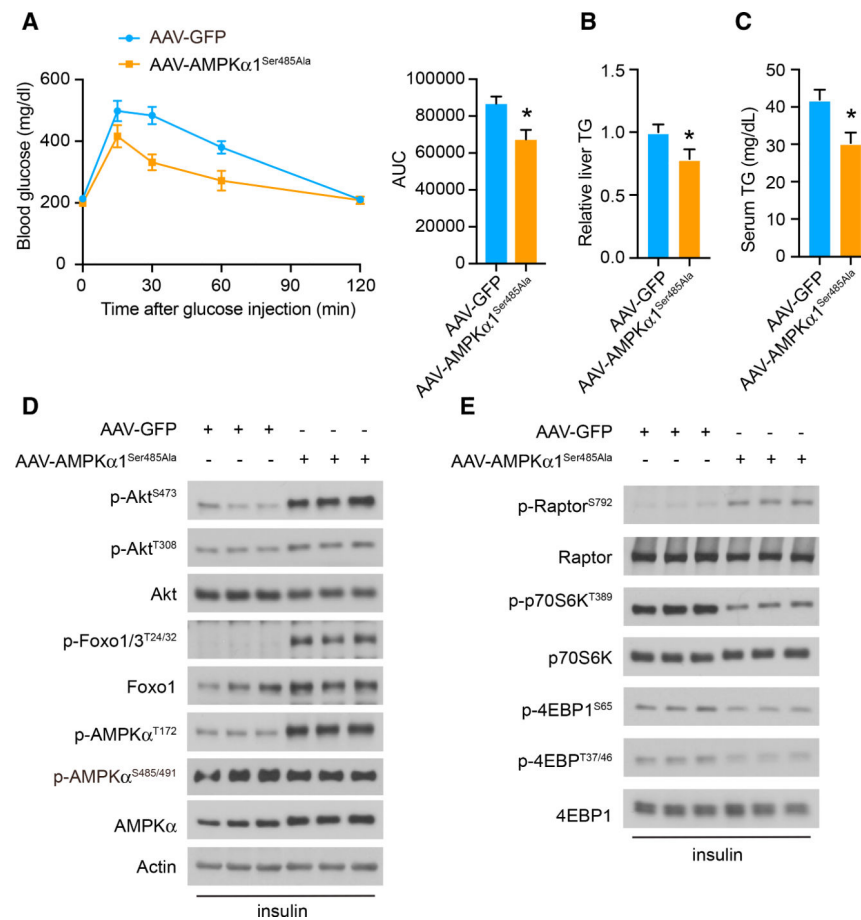


Figure 5. Liver-specific expression of AMPK α 1 lacking the inhibitory serine 485 phosphorylation site increases glucose tolerance and insulin sensitivity of HFD-fed mice
 (A) I.p. glucose tolerance tests with AAV-mediated expression of GFP or AMPK α 1^{Ser485Ala} (n = 7 wild-type male mice per group) under the liver-specific TBG promoter on HFD.
 (B and C) Liver TG (B) and serum TG (C) in wild-type mice with hepatic expression of GFP (n = 8) or AMPK α 1^{Ser485Ala} (n = 7 male mice).
 (D) Expression of AMPK α 1^{Ser485Ala} in liver enhances AMPK α 1^{Thr172} phosphorylation and hepatic insulin signaling through AKT and FoxO.
 (E) Expression of AMPK α 1^{Ser485Ala} in liver inhibits hepatic mTORC1 signaling.
 See also Figure S5 and Table S1 for information on mouse sex, age, n, and replication. *p < 0.05 by t test. All bars indicate mean and SEM.

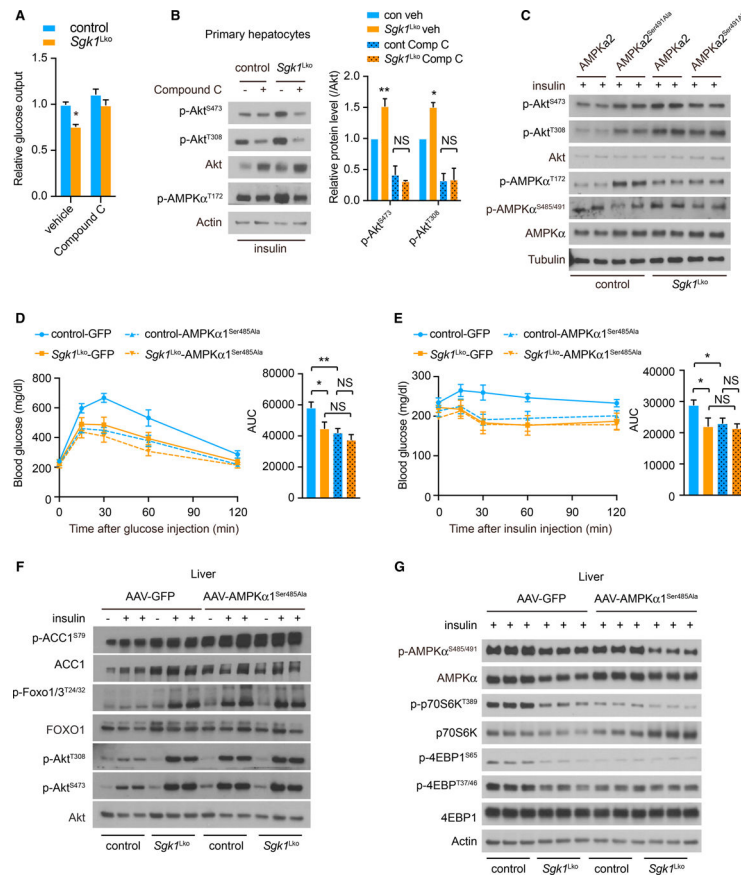


Figure 6. Hepatic SGK1 regulates systemic glucose homeostasis through AMPK

(A) AMPK inhibitor Compound C negates decreased glucose output in *Sgk1^{Lko}* primary hepatocytes (n = 9 replicates per group).

(B) Compound C eliminates increased Akt phosphorylation in *Sgk1^{Lko}* primary hepatocytes, quantified in the right panel (n = 3 replicates per group).

(C) Adenoviral-mediated expression of AMPK α 2^{Ser491Ala} increases insulin-stimulated Akt^{Ser473/Thr308} phosphorylation in control but not in *Sgk1^{Lko}* primary hepatocytes.

(D) I.p. glucose tolerance tests in control and *Sgk1^{Lko}* mice with hepatic overexpression of GFP or AMPK α 1^{Ser485Ala} (n = 7 for control;GFP, n = 10 for control;AMPK α ^{Ser485Ala}, n = 7 for *Sgk1^{Lko}*;GFP, n = 9 for *Sgk1^{Lko}*;AMPK α ^{Ser485Ala}).

(E) I.p. insulin tolerance tests in control and *Sgk1^{Lko}* mice with hepatic overexpression of GFP or AMPK α 1^{Ser485Ala} (n = 7 mice per group).

(F) Insulin-stimulated phosphorylation of Akt and Foxo in control and *Sgk1^{Lko}* mice with AAV-mediated hepatic overexpression of GFP or AMPK α 1^{Ser485Ala}.

(G) Phosphorylation of mTORC1 substrates S6K and 4EBP1 in control and *Sgk1^{Lko}* mice with hepatic overexpression of GFP or AMPK α 1^{Ser485Ala}.

See also Table S1 for information on mouse sex, age, n, and replication. *p < 0.05 and **p < 0.01 (NS, not significant) by two-way ANOVA (A, B, D, and E). All bars indicate mean and SEM.

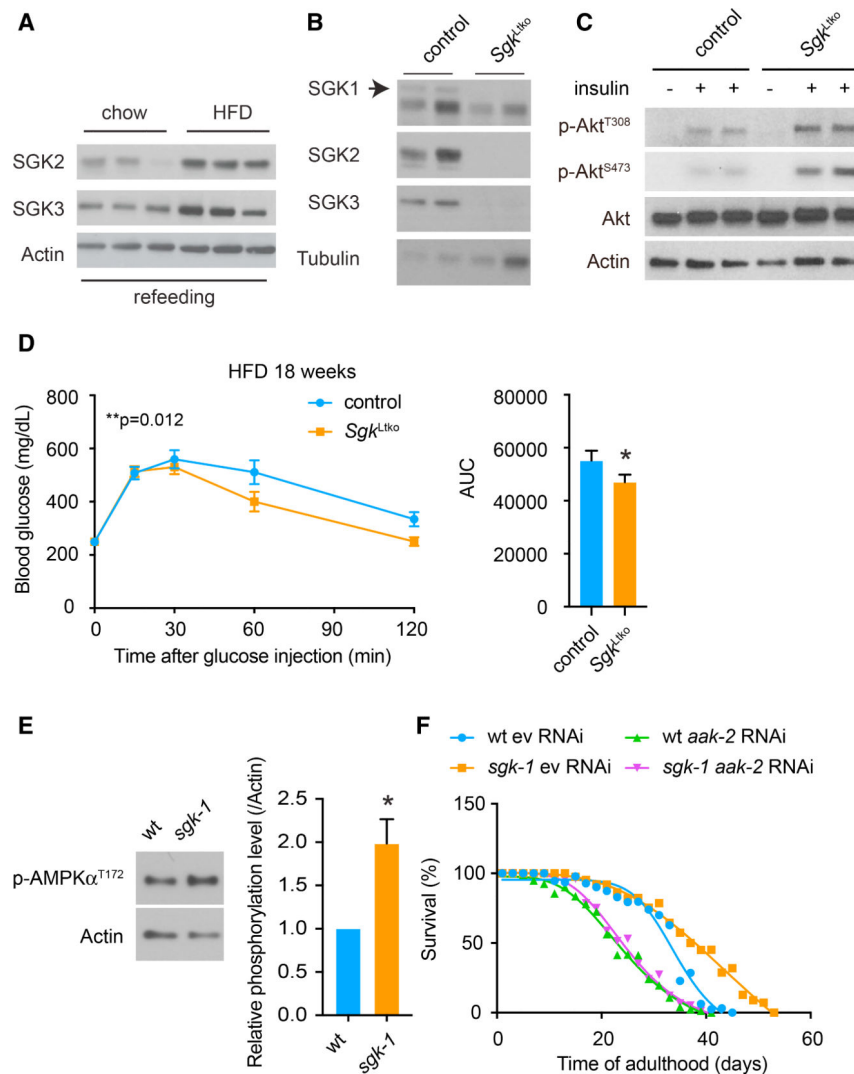


Figure 7. Improved glucose tolerance and insulin sensitivity in *Sgk^{Ltko}* mice
 (A) SGK2 and SGK3 western blot 2 h following refeeding after an overnight 16 h fast.
 (B) Hepatic knockout of *Sgk1*, *Sgk2*, and *Sgk3* validated by western blotting.
 (C) Insulin-stimulated Akt phosphorylation by western blotting in control and *Sgk^{Ltko}* primary hepatocytes.
 (D) I.p. glucose tolerance test in control (n = 11) and *Sgk^{Ltko}* (n = 13) mice fed a HFD.
 (E) AMPK phosphorylation in *sgk-1* mutant *C. elegans* under fed conditions at the young adult stage, quantified in the right panel versus actin (n = 3 biological replicates per group).
 (F) Extended starvation survival of *sgk-1* mutant worms is dependent on the AMPK α catalytic subunit *aak-2* (n = 60–90 animals per group per time point). Corrected p < 0.005 *sgk-1*(vector RNAi) versus wild-type(vector RNAi); corrected p < 0.005 *sgk-1*(vector RNAi) versus *sgk-1*(*aak-2* RNAi); and non-significant *sgk-1*(*aak-2* RNAi) versus wild-type(*aak-2* RNAi) for mean lifespan by nonlinear regression analysis.

See also Figure S6 and Table S1 for information on mouse sex, age, n, and replication. * $p < 0.05$ by t test (D and E) and p value as indicated by two-way ANOVA for effect by genotype (D, left panel). All bars indicate mean and SEM.

KEY RESOURCES TABLE

REAGENT or RESOURCE	SOURCE	IDENTIFIER
Antibodies		
Mouse monoclonal anti-Actin (C4)	Abcam	Cat# ab14128; RRID:AB_300931
Rabbit monoclonal anti-SGK1 (D27C11)	Cell Signaling Technology	Cat# 12103; RRID:AB_2687476
Rabbit monoclonal anti-SGK2 (D7G1)	Cell Signaling Technology	Cat# 7499; RRID:AB_10828732
Rabbit monoclonal anti-SGK3 (D18D1)	Cell Signaling Technology	Cat# 8156; RRID:AB_10949507
Rabbit monoclonal anti-HSP90 (C45G5)	Cell Signaling Technology	Cat# 4877; RRID:AB_2233307
Rabbit monoclonal anti-p70 S6 Kinase (49D7)	Cell Signaling Technology	Cat# 2708; RRID:AB_390722
Rabbit monoclonal anti-Phospho-p70 S6 Kinase (Thr389) (108D2)	Cell Signaling Technology	Cat# 9234; RRID:AB_2269803
Rabbit monoclonal anti-S6 Ribosomal Protein (5G10)	Cell Signaling Technology	Cat# 2217; RRID:AB_331355
Rabbit monoclonal anti-Phospho-S6 Ribosomal Protein (Ser240/244) (D68F8)	Cell Signaling Technology	Cat# 5364; RRID:AB_10694233
Rabbit monoclonal anti-Phospho-AMPK α (Thr172) (40H9)	Cell Signaling Technology	Cat# 2535; RRID:AB_331250
Rabbit polyclonal anti-Phospho-AMPK α 1 (Ser485)/AMPK α 2 (Ser491)	Cell Signaling Technology	Cat# 4185; RRID:AB_331250
Rabbit monoclonal anti AMPK α (D63G4)	Cell Signaling Technology	Cat# 5832; RRID:AB_10624867
Rabbit polyclonal anti-Phospho-4E-BP1 (Ser65)	Cell Signaling Technology	Cat# 9451; RRID:AB_330947
Rabbit monoclonal anti-Phospho-4E-BP1 (Thr37/46) (236B4)	Cell Signaling Technology	Cat# 2855; RRID:AB_560835
Rabbit monoclonal anti-4E-BP1 (53H11)	Cell Signaling Technology	Cat# 9644; RRID:AB_2097841
Rabbit monoclonal anti-Phospho-Akt (Ser473) (D9E) XP®	Cell Signaling Technology	Cat# 4060; RRID:AB_2315049
Rabbit monoclonal anti-Phospho-Akt (Thr308) (C31E5E)	Cell Signaling Technology	Cat# 2965; RRID:AB_2255933
Rabbit monoclonal anti-Akt (pan) (C67E7)	Cell Signaling Technology	Cat# 4691; RRID:AB_915783
Rabbit monoclonal anti-Phospho-FoxO1 (Thr24)/FoxO3a (Thr32)/FoxO4 (Thr28) (4G6)	Cell Signaling Technology	Cat# 2599; RRID:AB_2106814
Rabbit monoclonal anti-FoxO1 (C29H4)	Cell Signaling Technology	Cat# 2880; RRID:AB_2106495
Rabbit monoclonal anti-Phospho-NDRG1 (Thr346) (D98G11) XP®	Cell Signaling Technology	Cat# 5482; RRID:AB_10693451
Rabbit monoclonal anti-NDRG1 (D6C2)	Cell Signaling Technology	Cat# 9408; RRID:AB_11140640
Rabbit monoclonal anti-Raptor (24C12)	Cell Signaling Technology	Cat# 2280; RRID:AB_561245
Rabbit polyclonal anti-Phospho-Raptor (Ser792)	Cell Signaling Technology	Cat# 2083; RRID:AB_2249475
Rabbit polyclonal anti-Phospho-Acetyl-CoA Carboxylase (Ser79)	Cell Signaling Technology	Cat# 3661; RRID:AB_330337
Rabbit monoclonal anti-Acetyl-CoA Carboxylase (C83B10)	Cell Signaling Technology	Cat# 3676; RRID:AB_2219397
Bacterial and virus strains		
AAV8.TBG.PI.eGFP.WPRE.bGH	Penn Vector Core	AV-8-PV0146
AAV8.TBG.PI.AMPK α 1-S485A.WPRE.bGH	This study	N/A
Ad-LacZ	This study	N/A
Ad-SGK1-CA	A gift from Anthony Rosenzweig's lab, Harvard Medical School and Massachusetts General Hospital, Boston, MA, USA	N/A
Ad-AMPK α 2	This study	N/A
Ad-AMPK α 2-S491A	This study	N/A

REAGENT or RESOURCE	SOURCE	IDENTIFIER
Biological samples		
Mouse liver tissue from control, <i>Sgk1^{Lko}</i> , <i>Sgk1^{Lko}</i> mice	This paper	N/A
Chemicals, peptides, and recombinant proteins		
RNAzol® RT	Molecular Research Center	RN 190
Insulin	Sigma-Aldrich	I9278
Transferrin	Sigma-Aldrich	T3705
Selenium	Sigma-Aldrich	S9133
Wortmannin	Sigma-Aldrich	W1628
Dexamethasone	Sigma-Aldrich	D4902
Anti-FLAG® M2 Magnetic Beads	Sigma-Aldrich	M8823
8-CPT-cAMP	Enzo	BML-CN130
Compound C	Enzo	BML-EI369
Insulin Humulin_ R U-100 (For ITT)	Eli Lilly	N/A
Collagenase Type 1	Washington Biochemical	CLS-1
Lipofectamine 3000	Thermo Fisher	L3000015
Protein A Magnetic Beads	New England Biolabs	S1425
Critical commercial assays		
Ultra-Sensitive Mouse Insulin ELISA Kit	Crystal Chem	90080
Pierce BCA protein assay	Thermo Fisher	23225
Triglyceride (Infinity)	Thermo Fisher	TR22421
Total cholesterol (Infinity)	Thermo Fisher	TR13421
Amplex Red Glucose/Glucose Oxidase Assay Kit	Thermo Fisher	A22189
Experimental models: Cell lines		
Human: HEK293T	ATCC	CRL-3216
Mouse: AML12	ATCC	CRL-2254
Mouse: Primary hepatocytes	This paper	N/A
Experimental models: Organisms/strains		
Mouse: B6.Cg- <i>Sgk1</i> [<i>flox/flox</i>]	Fejes-Tóth et al., 2008	N/A; RRID: MGI:5317851
Mouse: B6.Cg- <i>Spee6-ps1^{Tg(Alb-cre)21Mgn}</i>]	The Jackson Laboratory	003574; RRID: IMSR_JAX: 003574
Mouse: B6.Cg- <i>Sgk1^{Lko}</i>	This study	N/A
Oligonucleotides		
<i>Sgk1</i> sgRNA targeting sequence: TAAGCAGCCGTATGACCGGA	This paper	N/A
<i>Sgk2</i> sgRNA targeting sequence: CGGAGCCTTCTACGCCGTGA	This paper	N/A
<i>Sgk3</i> sgRNA targeting sequence: CAAGGCACTGGCGATCTCCG	This paper	N/A
<i>Actin</i> qPCR primer, Forward: CTAAGGCCAACCGTGAAAAG	This paper	N/A

REAGENT or RESOURCE	SOURCE	IDENTIFIER
<i>Actin</i> QPCR primer, Reverse: GGGGTGTTGAAGGTCTCAA	This paper	N/A
<i>36b4</i> QPCR primer, Forward: AGATTCGGGATATGCTGTTGGC	This paper	N/A
<i>36b4</i> QPCR primer, Reverse: TCGGGTCTTAGACCAGTGTTTC	This paper	N/A
<i>Sgk1</i> QPCR primer, Forward: CTGCTCGAAGCACCCCTTACC	This paper	N/A
<i>Sgk1</i> QPCR primer, Reverse: TCCTGAGGATGGGACATTTTCA	This paper	N/A
<i>G6pase</i> QPCR primer, Forward: AGCAGTTCCTGTACCTGT	This paper	N/A
<i>G6pase</i> QPCR primer, Reverse: TGGCTTTTTCTTTCTCGAA	This paper	N/A
<i>Pepck</i> QPCR primer, Forward: TGCCTGGATGAAGTTTGATG	This paper	N/A
<i>Pepck</i> QPCR primer, Reverse: CGTTTTCTGGTTGATAGCC	This paper	N/A
<i>Pgc1a</i> QPCR primer, Forward: AATGCAGCGGTCTTAGCACT	This paper	N/A
<i>Pgc1a</i> QPCR primer, Reverse: ACGTCTTTGTGGCTTTTGCT	This paper	N/A
<i>Acc1</i> QPCR primer, Forward: GGACACCAGTTTTGCATTGA	This paper	N/A
<i>Acc1</i> QPCR primer, Reverse: AGTTTGGGAGGACATCGAAA	This paper	N/A
<i>Fasn</i> QPCR primer, Forward: GCACCTTTGATGACATCGTG	This paper	N/A
<i>Fasn</i> QPCR primer, Reverse: TCAGGTTTCAGTCCCACAGA	This paper	N/A
<i>Scd1</i> QPCR primer, Forward: CCTCCTGCAAGCTCTACACC	This paper	N/A
<i>Scd1</i> QPCR primer, Reverse: CAGAGCGCTGGTCATGTAGT	This paper	N/A
<i>Srebp1c</i> QPCR primer, Forward: GAGCCATGGATTGCACATTT	This paper	N/A
<i>Srebp1c</i> QPCR primer, Reverse: CGGGAAGTCACTGTCTTGGT	This paper	N/A
Recombinant DNA		
Flag-SGK1-WT	This paper	N/A
pCMV5-Flag	This paper	N/A
Flag-SGK1-S422D	This paper	N/A
Flag-SGK1-S422A	This paper	N/A
Software and algorithms		
ImageJ2	NIH	https://imagej.nih.gov/ij/
GraphPad Prism7	GraphPad Software, Inc.	http://www.graphpad.com/